

1 **Mannan detecting C-type lectin receptor probes recognise immune epitopes with**
2 **diverse chemical, spatial and phylogenetic heterogeneity in fungal cell walls**

3

4 Ingrida Vendele^{1,2}, Janet A. Willment¹, Lisete M. Silva³, Angelina S. Palma^{3,5}, Wengang Chai³,
5 Yan Liu³, Ten Feizi³, Mark H. T. Stappers^{1,4}, Gordon D. Brown¹ and Neil A. R. Gow^{1,4*}

6

7 Affiliations:

8 ¹MRC Centre for Medical Mycology, Aberdeen Fungal Group, College of Life Sciences and
9 Medicine, Institute of Medical Sciences, University of Aberdeen, Foresterhill, Aberdeen, AB25
10 2ZD, UK.

11 ² Division of Infection and Immunity, The Roslin Institute and Royal (Dick) School of Veterinary
12 Studies, University of Edinburgh, Edinburgh EH25 9RG, UK.

13 ³Glycosciences Laboratory, Department of Medicine, Imperial College London, Du Cane Road
14 W12 0NN, UK.

15 ⁴ School of Biosciences, University of Exeter, Geoffrey Pope Building, Exeter EX4 4QD, UK.

16 ⁵ UCIBIO, Department of Chemistry, Faculty of Science and Technology, NOVA University of
17 Lisbon, Lisbon, 2829, Portugal.

18

19 * corresponding author: n.gow@exeter.ac.uk

20

21 *Running title:* Fc-lectin mapping of fungal cells

22 *Keywords:* *Candida*, cell wall, C-type lectins, immune recognition, mannans, glycan
23 microarray

24

25

26

27

28

29 **Abstract**

30 During the course of fungal infection, pathogen recognition by the innate immune system is
31 critical to initiate efficient protective immune responses. The primary event that triggers
32 immune responses is the binding of Pattern Recognition Receptors (PRRs), which are
33 expressed at the surface of host immune cells, to Pathogen-Associated Molecular Patterns
34 (PAMPs) located predominantly in the fungal cell wall. Most fungi have mannosylated PAMPs
35 in their cell walls and these are recognized by a range of C-type lectin receptors (CTLs).
36 However, the precise spatial distribution of the ligands that induce immune responses within
37 the cell walls of fungi are not well defined. We used recombinant IgG Fc-CTLs fusions of three
38 murine mannan detecting CTLs, including dectin-2, the mannose receptor (MR) carbohydrate
39 recognition domains (CRDs) 4-7 (CRD4-7), and human DC-SIGN (hDC-SIGN) and the β -1,3
40 glucan-binding lectin dectin-1 to map PRR ligands in the fungal cell wall. We show that
41 epitopes of mannan-specific CTL receptors can be clustered or diffuse, superficial or buried
42 in the inner cell wall. We demonstrate that PRR ligands do not correlate well with phylogenetic
43 relationships between fungi, and that Fc-lectin binding discriminated between mannosides
44 expressed on different cell morphologies of the same fungus. We also demonstrate CTL
45 epitope differentiation during different phases of the growth cycle of *Candida albicans* and that
46 MR and DC-SIGN labelled outer chain *N*-mannans whilst dectin-2 labelled core *N*-mannans
47 displayed deeper in the cell wall. These immune receptor maps of fungal walls therefore reveal
48 remarkable spatial, temporal and chemical diversity, indicating that the triggering of immune
49 recognition events originates from multiple physical origins at the fungal cell surface.

50 **Author Summary**

51 Invasive fungal infections remain an important health problem in immunocompromised
52 patients. Immune recognition of fungal pathogens involves binding of specific cell wall
53 components by pathogen recognition receptors (PRRs) and subsequent activation of immune
54 defences. Some cell wall components are conserved among fungal species while other
55 components are species-specific and phenotypically diverse. The fungal cell wall is dynamic

56 and capable of changing its composition and organization when adapting to different growth
57 niches and environmental stresses. Differences in the composition of the cell wall lead to
58 differential immune recognition by the host. Understanding how changes in the cell wall
59 composition affect recognition by PRRs is likely to be of major diagnostic and clinical
60 relevance. Here we address this fundamental question using four soluble immune receptor-
61 probes which recognize mannans and β -glucan in the cell wall. We use this novel methodology
62 to demonstrate that mannan epitopes are differentially distributed in the inner and outer layers
63 of fungal cell wall in a clustered or diffuse manner. Immune reactivity of fungal cell surfaces
64 did not correlate with relatedness of different fungal species, and mannan-detecting receptor-
65 probes discriminated between cell surface mannans generated by the same fungus growing
66 under different conditions. These studies demonstrate that mannan-epitopes on fungal cell
67 surfaces are differentially distributed within and between the cell walls of fungal pathogens.

68

69 **Introduction**

70 Fungi are associated with a wide spectrum of diseases ranging from superficial skin and
71 mucosal surface infections in immunocompetent people, to life-threatening systemic infections
72 in immunocompromised patients [1, 2]. The global burden of fungal infections has increased
73 due to infection related or medically imposed immunosuppression, the use of broad-spectrum
74 antibiotics that suppress bacterial competitors, and the use of prosthetic devices and
75 intravenous catheters in medical treatments [3, 4]. Patients that are pre-disposed to fungal
76 diseases include those with neutropenia, those undergoing stem cell or organ transplant
77 surgery or recovering from surgical trauma as well as HIV infected individuals and those with
78 certain rare predisposing mutations in immune recognition pathways [3-6].

79 Innate immunity is the primary defence mechanism against fungal infections and involves host
80 Pattern Recognition Receptors (PRRs) that recognise specific Pathogen-Associated
81 Molecular Patterns (PAMPs), which are mostly located within the cell wall [7-9]. These

82 receptor-ligand interactions are the primary origin of all immune responses and they promote
83 expression and secretion of various chemokines and cytokines that results in recruitment of
84 neutrophils, macrophages and other immune cell types to the site of infection, which ultimately
85 leads to containment and clearance of the pathogen and the activation of protective longer
86 term adaptive immunity [9-12].

87 The repertoire of ligands in fungal cell walls that engage with cognate PRRs has been
88 reviewed extensively [13-15] but we lack information about where precisely these ligands are
89 located in the fungal cell wall. Most fungi have a two layered cell wall with an inner layer
90 comprised of a conserved glucan-chitin scaffold to which a diversity of outer cell wall
91 components are attached that varies significantly between different fungal species [14-16]. In
92 *Candida* species the outer wall is dominated by a fibrillar layer of highly glycosylated cell wall
93 proteins that are extensively decorated with *N*- and *O*-linked mannans and phosphomannans
94 [17, 18]. The chemical fingerprint of the fungal cell wall mannans are used to identify medically
95 relevant species in diagnostic tests [19-21]. However, within a species the composition of the
96 cell wall is highly variable and changes according to morphology, growth stage, nutrient
97 availability, the presence of antibiotics and other environmental stressors [15, 22-25]. This
98 chemical and architectural plasticity represents a moving target for the immune system and
99 leads to differential immune activation at different stages of an infection [25]. Understanding
100 the relationship between fungal cell wall composition and immune recognition is therefore
101 critically important in fungal pathogenesis and immunity and in the context of fungal
102 diagnostics, vaccines and immunotherapies [26-28].

103 C-type Lectin (CTL) receptors orchestrate antifungal immunity through recognition of fungal-
104 specific ligands that are mainly located in the cell wall [29-33]. Multiple CTLs participate in
105 pathogen recognition of fungal cell wall components including β -glucan, chitin, mannans and
106 melanin [34-40]. Dectin-1 recognises β -1,3-glucan that is a conserved element of the inner
107 cell wall of all known fungal pathogens [41, 42]. Mannans are more complex, comprising linear
108 and branched polymers of mannose sugars linked via α -1,2, α -1,3, α -1,4, α -1,6, and β -1,2

109 glycosidic bonds that may be further modified by phosphodiester side chains [18, 43, 44].
110 These glycosides decorate the cell wall proteins of the outer cell walls and the integral proteins
111 in the cell membrane and may account for more than 80% of the mass of the glycoprotein [18,
112 43, 44]. A wide range of mannan-recognising immune receptors are present in myeloid and
113 epithelial cells including the mannose receptor (MR), dectin-2, dectin-3, mincle, DC-SIGN,
114 galectin-3, FcγR, CD14, CD23, TLR2, TLR4 and TLR6 [13, 34, 37, 45-54]. The number and
115 diversity of mannan-recognising PRRs underlines their importance in primary immune
116 recognition events. Although these recognition events are the primary trigger of the immune
117 response, the precise chemical nature and location of the ligands that are recognised by these
118 immune receptors has not been investigated in detail.

119 We utilized murine CTL receptor carbohydrate recognition domains and human IgG Fc fusion
120 proteins (Fc-lectins) including dectin-2, MR CRD4-7, dectin-1 and acquired commercial
121 human DC-SIGN-Fc to explore the distribution of mannan- and β-glucan- detecting CTLs [36,
122 37, 55]. We used the murine MR cysteine rich (CR) domain fused to human IgG Fc to control
123 for Fc mediated binding events [56, 57]. The CR lacks the carbohydrate recognition domains
124 and binds to untreated sulphated carbohydrates. These Fc-lectin probes were used to
125 examine the distribution of immune epitopes in fungal cell surfaces and to examine the nature
126 of the ligand engaging with specific mannan-detecting CTLs. We reveal remarkable diversity
127 in the location and distribution of the cognate immune ligands and demonstrate that these
128 ligands bind different mannans in different parts of the cell wall in order to induce immune
129 responses.

130

131 **Results**

132 **Distribution of C-type lectin receptor ligands on fungal cell surfaces**

133 We first confirmed the ability of a set of Fc-lectins to bind their cognate target antigens by
134 ELISA using whole yeast *C. albicans* cells, purified *S. cerevisiae* mannan and *Candida* yeast

135 β -glucan (S Fig. 1 A) and verified the molecular weight of the recombinant Fc-lectins (S Fig. 1
136 B). The Fc region did not influence binding since the control protein CR-Fc lacking the MR
137 carbohydrate binding domains did not recognise any of the immobilised targets (S Fig. 1 A).
138 Binding of the various Fc-lectins against reported mannan or β -1,3 glucan targets and Fc-
139 probe integrity was therefore confirmed.

140 We then examined variability in expression and distribution of epitopes for CTL receptors in a
141 range of fungal strains and species (Fig. 1). CTL Fc-lectins bound different yeast cells with
142 differing intensities and patterns (Fig. 1 A-C). MR probe (CRD4-7-Fc) and dectin-2-Fc labelled
143 *C. glabrata* and *C. krusei* more strongly than *C. parapsilosis* (Fig. 1 A, B), however there was
144 no clear correlation between the profiles of Fc-lectin binding and the phylogenetic relatedness
145 of the species. For example, *C. albicans* and *C. dubliniensis* are relatively close genetic
146 relatives yet displayed very different CTL binding profiles (Fig. 1 A, B). *C. dubliniensis*
147 demonstrated higher binding by dectin-2-Fc and CRD4-7-Fc compared to *C. albicans* (Fig. 1
148 A, B), and mannose receptor probe (CRD4-7-Fc) bound *C. dubliniensis* more diffusely whilst
149 dectin-2-Fc binding was not visible by fluorescence microscopy on *C. albicans* yeast cell walls
150 but labelled *C. dubliniensis* yeast cells in a punctate pattern (Fig. 1 C).

151 Three virulent (SC5314, Ysu751, J990102) and three attenuated (IHEM3742, AM2003/0069,
152 HUN92) isolates of *C. albicans* were examined, as determined in both mouse and insect
153 systemic models of infection [58, 59]. There was no clear relationship between binding of
154 dectin-2-Fc, CRD4-7-Fc and dectin-1-Fc probes and virulence except that attenuated yeasts
155 exhibited a tendency to higher binding of dectin-2-Fc (Fig. 2 A). However, strain CAI4-CIp10
156 [60], which is the genetic background for the generation of multiple *C. albicans* null mutants
157 and its progenitor clinical isolate SC5314 exhibited identical Fc-lectin binding patterns (Fig. 2
158 A). In *C. albicans* hyphae, similar Fc-lectin binding patterns were observed for all strains,
159 however, the attenuated HUN92 isolate was a high dectin-2-Fc binder with most labelling
160 occurring at the hyphal tips (Fig. 2 B). Therefore, the Fc-lectins demonstrated differing binding

161 profiles to different *Candida* species and *C. albicans* strains with no clear association between
162 Fc-lectin binding, phylogenetic relatedness and relative virulence.

163 **Differential expression of ligands for C-type lectin receptors during growth and**
164 **morphogenesis**

165 We next tested the stability of the epitopes recognised by CTL-Fc-lectins during the growth
166 and morphogenesis of *C. albicans*. Samples in the lag phase, early, mid and late exponential
167 as well as stationary phases were sampled during batch growth (Fig. 3 A). During the period
168 of exponential growth of yeast cells, dectin-2-Fc ligand exposure was somewhat reduced (Fig.
169 3 B) whilst β -glucan for dectin-1-Fc was increased (Fig. 3 B). In contrast, epitopes for mannose
170 receptor assessed by CRD4-7-Fc binding appeared to be exposed throughout all growth
171 phases of batch growth (Fig. 3 B). Therefore PAMP binding was affected by growth phase and
172 potentially growth rate of the target pathogen.

173 *C. albicans* filamentation was induced and hyphal cells were fixed at different time points to
174 test Fc-lectin binding (Fig. 4). Mannan-recognising dectin-2-Fc and CRD4-7-Fc demonstrated
175 strong binding to early germ tubes grown in serum-containing medium (Fig. 4 A, B). However,
176 binding of both mannan-detecting lectin probes gradually decreased over prolonged periods
177 of hyphal growth (Fig. 4 A, B). In particular, decreasing binding of CRD4-7-Fc to the mother
178 yeast cell was observed and was virtually absent on germ tubes that were older than 2 h (Fig.
179 4 B). In contrast, although germ tubes lacked bud scars, which have exposed β -1,3 glucan,
180 dectin-1-Fc demonstrated the opposite pattern with binding gradually increasing to the lateral
181 cell walls of maturing filamentous cells (Fig. 4 C). These results reinforce previous
182 observations that nascent mannan epitopes are gradually modified as the yeast cells and
183 hyphae progress through different growth stages [61].

184 The binding of mannan-detecting C-type lectins to yeast, pseudohypha, hypha and the
185 recently described goliath cells [62] of *C. albicans* was examined (Fig. 5). Dectin-2-Fc
186 demonstrated low binding affinity to *C. albicans* fixed yeast cells which could be detected by

187 flow cytometry (Fig. 1-3) but not by microscopy (Fig. 5 A). Fixation was used to capture and
188 immobilise cells at specific morphogenetic stages, but control experiments showed that
189 paraformaldehyde fixation did not influence Fc-lectin binding patterns (data not shown).
190 Dectin-2-Fc exhibited punctate binding pattern on hyphae with strong staining observed at the
191 hyphal tip (Fig. 5 A). In contrast, CRD4-7-Fc demonstrated high intensity punctate binding to
192 both yeast cells and hyphae (Fig. 5 B). As predicted, dectin-1-Fc recognised yeast cells mainly
193 at the bud scars while some punctate binding was also detected along hyphae (Fig. 5 C) [63].
194 All Fc-lectins recognised pseudohypha cells with intermediate binding strengths compared to
195 that for yeast and hyphae (Fig. 5 A-C). Recently, goliath cells have been observed as a form
196 of cellular gigantism in *Candida* species [59]. Fc-lectin binding to *C. albicans* goliath cells
197 revealed punctate dectin-2-Fc binding while CRD4-7-Fc bound more uniformly around the cell
198 surface (Fig. 5). As before, dectin-1-Fc bound mainly to the bud scars of goliath cells (Fig. 5).
199 Negative control protein CR-Fc did not show any binding to any of the *C. albicans*
200 morphologies (Fig. 5 D), and binding to yeast cells was not detected by flow-cytometric
201 analyses. These data demonstrated differences in the specificities of dectin-2-Fc and CRD4-
202 7-Fc towards the fungal cell surface components, and were in accord with knowledge of the
203 glycan-binding specificities of dectin-1 [64] and of CR-Fc [57].

204 **Spatial distribution of mannan epitopes in the inner cell wall**

205 To elucidate precise localisation of ligands for mannan-recognising Fc-lectins within the cell
206 wall, immunogold labelling of dectin-2-Fc, CRD4-7-Fc and CR-Fc-stained embedded sections
207 of cells was analysed by TEM (Fig. 6). We observed clustered dectin-2-Fc binding to both
208 yeast and hyphae inner cell walls of *C. albicans* with little labelling of the outer mannoprotein-
209 rich fibrils (Fig. 6 A). CRD4-7-Fc recognised ligands within the plasma membrane as well as
210 outer glycoprotein fibrils (Fig. 6 B). CR-Fc gave no staining (Fig. 6 C). The differential
211 specificities of dectin-2-Fc, CRD4-7-Fc and CR-Fc recognition were again demonstrated.
212 Flow cytometry and microscopy were used to compare binding strengths of Fc-lectins to
213 *C. albicans* yeast cell wall after mild heat treatment (at 65°C) which mechanically perturbs the

214 normal cell wall architecture resulting in the permeabilising of the wall to otherwise
215 impermeable high molecular weight components (Fig. 7). This mild heat treatment is often
216 used to heat-kill (HK) cells to prevent cellular morphogenesis during immunological
217 examinations. Binding affinities of dectin-2-Fc, CRD4-7-Fc and dectin-1-Fc to formaldehyde-
218 fixed or HK *C. albicans* yeast cells were compared (Fig. 7 A-C). Dectin-2-Fc binding increased
219 significantly following HK treatment (Fig. 7 A) while CRD4-7-Fc binding was reduced to a minor
220 extent (Fig. 7 B), suggesting that the CRD4-7-Fc MR ligand was superficial whilst the dectin-
221 2 ligand was buried deeper in the cell wall and was initially inaccessible to CTLs. HK also
222 increased binding of dectin-1-Fc, due to β -glucan exposure (Fig. 7 C). The specificity of Fc-
223 lectin binding was further corroborated by blocking the binding of the Fc-lectins with purified
224 *C. albicans* cell wall mannan (dectin-2-Fc and CRD4-7-Fc) or yeast cell wall β -glucan (dectin-
225 1-Fc) (Fig. 7 A-C). In all cases external addition of an excess of the target polysaccharide
226 completely blocked the binding of Fc-lectins to the cell wall. CR-Fc included as a negative
227 control again showed that binding to fixed or HK cells was not mediated by the Fc region of
228 the CTL-probes (Fig. 7 A-C). Collectively these analyses revealed that some CTL epitopes
229 were clustered in the cell wall whilst others were uniformly distributed and some were exposed
230 and some cloaked within the inner cell wall.

231 **hDC-SIGN epitopes in the plasma membrane and cell wall**

232 Human DC-SIGN-Fc recombinant protein (Life Technologies) was used to further investigate
233 mannan epitope variability on the fungal surface. hDC-SIGN-Fc consistently demonstrated
234 high affinity binding of *C. albicans* fixed yeast cells (Fig. 8 A) whereas with HK yeast cells there
235 was a significant decrease in hDC-SIGN-Fc binding (Fig. 8 A). Binding was completely blocked
236 in the presence of purified and soluble *C. albicans* mannan (Fig. 8 A, B) and decreased by
237 75% when using *S. cerevisiae* mannan (Fig. 8 B). Microscopy revealed a high intensity
238 punctate binding pattern on yeast, hyphae and goliath cells and slightly less to pseudohyphal
239 *C. albicans* cells (Fig. 8 C). Using immunogold-labelling hDC-SIGN-Fc epitopes were
240 observed in the plasma membrane, inner cell wall and outer fibrils for yeast and hyphae of

241 *C. albicans* (Fig. 8 D) that was similar to that observed for CRD4-7-Fc labelling. The binding
242 to hDC-SIGN-Fc epitopes progressively decreased in maturing, more elongated *C. albicans*
243 hyphae (Fig. 8 E). Reminiscent of CRD4-7-Fc binding, hDC-SIGN-Fc demonstrated high
244 intensity binding to *C. albicans* cells in different morphologies with binding sites distributed
245 along the plane of the plasma membrane and in the outer cell wall glycosylated fibril layer.

246 **Chemical nature of C-type lectin receptor targets in fungal cell walls**

247 To assess the nature of the targets of the CTL receptors, the binding of the Fc-lectin probes
248 was examined using a collection of cell wall mutants including isogenic nulls with truncations
249 in *N*- and *O*-mannans (Fig. 9). In general, mannosylation mutants exhibited marked changes
250 in Fc-lectin recognition. The *C. albicans mnn4Δ* mutant lacks phosphomannosyl residues and
251 consequently these mutants have uncharged cell walls [65]. The *mnn4Δ* demonstrated
252 increased binding of dectin-2-Fc, reduced binding of CRD4-7-Fc and a similar binding profile
253 of hDC-SIGN-Fc compared to SC5314 (Fig. 9 A). The *N*-mannan outer chain mutant *mnn2-*
254 *26Δ* that lacks *N*-mannan side chains demonstrated a slight increase in dectin-2-Fc, reduced
255 CRD4-7-Fc and a similar binding profile of hDC-SIGN-Fc compared to SC5314 (Fig. 9 A) [66].
256 An *N*-mannan mutant *och1Δ*, with no outer *N*-linked mannan chains and a markedly reduced
257 phosphomannan content but increased chitin and glucan [67], resulted in much higher binding
258 of dectin-2-Fc, CRD4-7-Fc and a dense binding pattern all over the yeast cell of hDC-SIGN-
259 Fc compared to SC5314 (Fig. 9 A). Increased binding of some *N*-mannan Fc-lectins to
260 mannosylation mutants can be explained by the compensatory synthesis of PRR-binding
261 epitopes as a consequence of the mutation [67]. A *pmr1Δ* mutant with reduced
262 phosphomannan, *O*-mannan and *N*-mannan [68] demonstrated marginally increased
263 recognition by dectin-2-Fc and reduction of CRD4-7-Fc and similar binding of hDC-SIGN-Fc
264 compared to wild type (Fig. 9 A). This is compatible with previous observations that dectin-2-
265 Fc recognised inner cell wall mannans whilst CRD4-7-Fc labelled the outer mannoprotein
266 fibrillar layer (Fig. 6 A, B). Dectin-1-Fc was used as a control and demonstrated increased
267 binding in all backgrounds deficient in *N*- and *O*-mannan attributable to the increased exposure

268 of inner cell wall component β -glucan (Fig. 9 A). Therefore, the cell wall glycosylation status
269 had a major impact on the ability of CTL probes to bind *C. albicans*.

270 To gain further insight into the carbohydrate recognition by the CTL receptors, we analysed
271 these initially using a microarray comprised mostly of fungal-type saccharides and compared
272 their binding profiles (Fig. 10, S Table 2). Both CRD4-7-Fc and hDC-SIGN-Fc showed strong
273 binding to the *C. albicans* *N*-mannoprotein that is characterised by an α -1,6-mannose
274 backbone with oligomeric α -1,2-, α -1,3-, and β -1,2-manno-oligosaccharide branches (Fig. 10
275 A, B, position 13, S Table 2). The two proteins bound also to other mannan-related
276 saccharides from *S. cerevisiae* and *M. tuberculosis*, that share an α 1,6-mannose backbone
277 with α -1,2-manno-oligosaccharide branches (Fig. 10 A, B, S Table 2). In contrast, no binding
278 was detected with dectin-2-Fc to any of Man α -1,2-Man-containing polysaccharides in the
279 conditions of the microarray analysis, which suggests it may have less capacity to bind α -
280 mannans of this type compared to CRD4-7-Fc and hDC-SIGN-Fc (data not shown). Dectin-1-
281 Fc showed, as predicted, strong and highly specific binding to glucans with a β -1,3-glucosyl
282 backbone (Fig. 10 C, S Table 2).

283 Glycan microarrays of 474 sequence-defined oligosaccharide probes (S Table 3 B) were also
284 applied to compare the binding specificities of dectin-2-Fc, CRD4-7-Fc and hDC-SIGN-Fc.
285 The signal intensities observed with dectin-2-Fc were the lowest overall among the three Fc
286 probes. Dectin-2-Fc binding was detected to Man₉GN₂ derived probes that resemble the core
287 *N*-mannan structures within the inner *C. albicans* cell wall (Fig. 11 A, S Table 3 A); this
288 relatively weak and restricted binding is in agreement with previous glycan array studies [37,
289 69]. No binding of dectin-2-Fc was detected to oligo-mannose sequences smaller than
290 Man₇GN₂. Additionally, binding was detected of dectin-2-Fc to 3'sialyl LNFPIII and a number
291 sulphated glycans as with hDC-SIGN-Fc.

292 CRD4-7-Fc showed mannose-related binding of high intensity to oligo/high-mannose *N*-glycan
293 sequences, fucosylated probes including Fuc-GlcNAc and Man₃FGN₂, as well as β -1,4-
294 oligomannoses (Fig. 11 B, S Table 3 A). hDC-SIGN-Fc gave strong binding signals with *N*-

295 acetylglucosamine containing sequences including chitin-derived glycans (Fig. 11 C, S Table
296 3 A) and also to glucan oligosaccharide sequences with differing glucosyl linkages as was
297 also observed in recent studies [70, 71] (Fig. 11 C, S Table 3 A)]. hDC-SIGN-Fc also gave
298 binding to a broad range of *N*-glycans including oligo/high-mannose sequences having α -1,2-
299 , α -1,6- and α -1,3/1,6-linked mannose, high-mannose sequences capped by Glc residues and
300 a number of *N*-acetylglucosamine-terminating *N*-glycans; binding was also detected to β 4-
301 linked mannose oligosaccharides as with CRD4-7-Fc. Collectively, glycan array binding
302 results are consistent with the dectin-2-Fc ligand being based on Man₉GN₂ found in the core
303 *N*-mannan triantennary structure within the *C. albicans* inner cell wall, whereas CRD4-7-Fc
304 and hDC-SIGN-Fc have a broader binding profile compared to dectin-2-Fc and can recognise
305 oligo-mannose structures terminating in α -1,3 and α -1,6- mannose resembling to some extent
306 those found in the outer-chain mannan structures. This is compatible with the binding patterns
307 observed using colloidal-gold TEM.

308

309 **Discussion**

310 CTL receptors provide a first line defence against fungal pathogens and orchestrate both
311 innate and adaptive immunity through the recognition of fungal PAMPs. A large number of
312 CTL receptors have been proposed to bind fungal cell wall epitopes such as mannans, β -1,3-
313 glucan and chitin [34, 37, 47, 50, 52]. Previous studies suggested dectin-2 to recognise high
314 mannose residues that are present on fungal cell surfaces while MR was proposed to bind
315 branched *N*-mannan structures, with fucose, *N*-acetylglucosamine sugar residues and
316 mannose-capped lipoarabinomannan (ManLAM) on the mycobacterial cell wall [34, 37, 72].
317 hDC-SIGN has been demonstrated to recognise galactomannan, mannose- and fucose-
318 containing glycoconjugates and *N*-linked mannose rich components in *C. albicans* cell wall
319 [38, 73]. There is however limited knowledge of the structural arrangement, spatial distribution
320 and variation in mannoside architecture of the cell wall of fungal pathogens, which this study
321 addresses. We deployed recombinant CTL-Fc proteins as probes to explore the distribution,

322 regulation and chemical structure of fungal ligands for these receptors within the cell wall, in
323 particular for dectin-2, MR and hDC-SIGN. We demonstrated that there is considerable intra-
324 and inter-species variability in the expression of key mannan epitopes. We mapped the
325 patterns of binding to these ligands during growth and cellular morphogenesis and observed
326 marked spatial segregation and an unexpected clustering of certain mannan epitopes.

327

328 The analysis of *C. albicans* cell wall mutants corroborated the occurrence of inner cell wall
329 epitopes for dectin-2-Fc and superficial mannan ligands for MR and hDC-SIGN-Fc. An *och1Δ*
330 mutant, which has a defect in its ability to synthesise outer chain *N*-glycans, had been shown
331 previously to have exposed inner cell wall components [67]. This mutant also exhibited
332 increased binding by dectin-2-Fc and has been shown to have an elaborated α -1,2- and α -
333 1,3-mannan side chains to the $\text{Man}_8\text{GlcNAc}_2$ core triantennary complex which is a ligand that
334 promotes CRD4-7-Fc and hDC-SIGN-Fc binding. Other mutants with decreased *N*-mannan
335 outer chains, including *mnn2-26Δ*, *pmr1Δ* [66, 68] bound less CRD4-7-Fc and hDC-SIGN-Fc
336 and more dectin-2-Fc commensurate with an increased exposure of the inner wall layers.
337 Moreover, the *mnn4Δ* mutant, which lacks cell wall phosphomannan that confers a negative
338 charge on the wall [65] had reduced binding by CRD4-7-Fc and hDC-SIGN-Fc but increased
339 dectin-2-Fc affinity. These observations complement previous studies suggesting that cell
340 surface glycosylation profoundly influences the efficiency of pathogen recognition by immune
341 receptors [9, 11, 13, 23, 74]. Glycan microarray data with the Fc-lectins and the fungal-type
342 saccharides are consistent with CRD4-7-Fc and hDC-SIGN-Fc but not dectin-2-Fc recognizing
343 α -1,6-Man backbone with oligomeric α -1,2-, α -1,3-, and β -1,2-Man branches which comprise
344 *C. albicans* outer wall *N*-mannan branches. This contrasts with the weak binding detected of
345 dectin-2-Fc to the high-mannose Man_9GN_2 probe with terminal $\text{Man}\alpha$ -1,2-Man sequences,
346 which resembles *C. albicans* core *N*-mannan within the inner cell wall. This is in agreement
347 with published data that showed the $\text{Man}\alpha$ -1,2-Man sequence on the Man_9GN_2 to be a primary
348 target for dectin-2 binding [37, 69], and that this receptor could adopt a geometry of the binding
349 site that accommodates the internal residues of the $\text{Man}\alpha$ -1,2- $\text{Man}\alpha$ -1,2-Man- (D1 branch)

350 and Man α -1,2-Man α -1,3-Man- (D2 branch) trisaccharide sequences [37, 69]. This prompts a
351 hypothesis that dectin-2 binds to internal sequences in fungal mannan polysaccharides,
352 expressing higher density of the ligands and achieving multivalent binding.

353 We examined the immunological signature of clinically-relevant *Candida* species and
354 *S. cerevisiae* and demonstrated that there was no simple correlation between phylogenetic
355 relationships between fungal species and CTL epitope distribution. Despite *C. albicans* and
356 *C. dubliniensis* sharing approximately 95% genome identity [75] the patterns of CTL probe
357 binding contrasted markedly. The immunologically relevant mannan structures are produced
358 by activities of multiple families of mannosyltransferases, of which genetic variation and
359 regulation may not map simply to phylogenetic relationships. We focused mainly on
360 *C. albicans* as the model organism for further mapping of cell wall dynamics. Previous studies
361 demonstrated that dectin-1 recognition of *C. albicans* was influenced by fungal strain type
362 because chitin levels modulated the accessibility of dectin-1 ligands [76]. Analogously, binding
363 of mannan-recognising CTL probes varied in different *C. albicans* strains and species.
364 Previous studies have identified virulent and attenuated isolates of this organism [58, 59],
365 however, Fc-lectin probes recognised both virulent and avirulent strains with similar binding
366 patterns and there was no simple correlation between virulence and CTL probe binding (Fig.
367 2 A). Previous studies have also demonstrated a strong correlation between the capacity to
368 form hyphae and virulence [77-81]. The intensity and distribution of mannan-specific CTL
369 binding to hyphae was found to vary during hypha elongation. It is possible that the efficiency
370 by which invading hyphae induce or escape immune surveillance ultimately influences
371 virulence.

372 We also demonstrated that *C. albicans* growth phase influenced expression and exposure of
373 cell wall components. Batch growth of *C. albicans* yeast culture revealed increased dectin-1-
374 Fc binding during the exponential growth phase. This is likely to be due to increased β -glucan
375 exposure and number of bud scars on actively dividing cells. As batch culture of cells
376 transitioned into the stationary phase, a reduction in dectin-1-Fc and increased dectin-2-Fc

377 binding was observed that was likely to be related both to the degree of mannan shielding of
378 β -glucan as the cell wall was reorganised. CRD4-7-Fc demonstrated similar binding patterns
379 during all growth phases of the yeast batch culture, highlighting the diversity in availability of
380 the cell wall manno-oligosaccharide sequences and suggesting that the CRD4-7-Fc (mannose
381 receptor) ligand is superficial in the cell wall. This suggestion was supported by colloidal gold-
382 TEM images showing CTL binding patterns at the ultrastructural level, and is in accord with a
383 previous study which demonstrated that MR was not required for host defence in a systemic
384 candidiasis mouse model [82].

385 The hyphal cell wall is also modified during the process of hyphal extension [17, 61]. In this
386 study we mapped the distribution of CTL epitopes on hyphal cell walls over a period of
387 prolonged hyphal growth and demonstrated that dectin-2-Fc and CRD4-7-Fc ligands were
388 densely concentrated at the emerging germ tube apex. Previous studies on *C. albicans*
389 suggested that mannan-recognising dectin-2 is a hypha-specific CTL [49], however, we
390 demonstrate here that the distribution and expression of dectin-2 epitopes on yeast cells
391 varies between different *Candida* species. There was little availability of dectin-1-Fc ligands
392 and by inference β -1-3 glucan on hyphae, possibly because of the lack of bud scars on hyphae
393 as discussed below. This supports previous studies describing attenuated dectin-1 activation
394 by hyphal cells [63]. As hyphae elongated, binding of mannan-recognising probes dectin-2-Fc
395 and CRD4-7-Fc was reduced and became more punctate while binding of dectin-1-Fc to
396 lateral cell walls increased. This finding supports observations that have demonstrated that β -
397 glucan becomes exposed late during disseminated *C. albicans* infection [61]. Interestingly,
398 binding of CRD4-7-Fc to *C. albicans* germinating cells demonstrated a reduction in mother
399 yeast cell recognition as the germ tube elongated. It is possible that the mannosylated
400 structures on yeast cell mannoproteins are chemically modified during hyphal elongation so
401 they are less able to be recognised by the MR. However, multiple mannan-detecting PRRs
402 were able to bind each of the various cell types of *C. albicans* that were studied. This
403 redundancy in CTL engagement presumably confers advantage in recognising fungal

404 pathogens whose surfaces and shapes are remodelled in response to host invasion and
405 colonisation of different microenvironments.

406 Morphological alterations of *C. albicans*, and other fungal pathogens, is often correlated with
407 their ability to thrive within the human host [83]. These cellular transitions are coupled to
408 changes in their cell wall composition which makes them a moving target for immune detection
409 [25, 84, 85]. *C. albicans* forms cells that are more or less elongated [83]. Synchronously
410 dividing elongated yeast cells (pseudohyphae) are considered by many to be a distinct cell
411 form, and these cell types are common to all *Candida* species. The tested Fc-lectin probes
412 also demonstrated intermediate binding affinities to pseudohyphae of *C. albicans* (Fig. 4),
413 complementing a recent study describing intermediate cytokine profiles to *C. albicans*
414 filamentous forms [86]. Goliath cells are recently recognised as an enlarged cell type of
415 *C. albicans* that may play an important role in commensalism and persistence in the gut [62].
416 We observe that dectin-2-Fc weakly recognises *C. albicans* yeast cells but has increased
417 binding on goliath cells (Fig. 4 A), potentially due to cell expansion and concomitant exposure
418 of inner cell wall epitopes or a novel arrangement of mannoproteins on the surfaces of goliath
419 cells that may expose more dectin-2-recognising mannan epitopes. Dectin-2-Fc also bound
420 well to hyphae of *C. albicans*, in particular at the hyphal tip (Fig. 4 A). The cell wall of the
421 hyphal apex is thinner and the polysaccharides are less crystalline and less cross-linked. This
422 may facilitate access of high molecular weight PRRs to inner cell wall ligands. Both mannose
423 receptor (CRD4-7-Fc) and hDC-SIGN-Fc probes demonstrated similar binding to different
424 morphologies and their binding was not greatly affected by mild heat treatments suggesting
425 their epitopes are superficial. As predicted, dectin-1-Fc binding was concentrated at the bud
426 scars of yeast and goliath cells, but binding was punctate on hyphal cells that lack bud scars.
427 Punctate binding patterns have been reported elsewhere, in particular for dectin-1 binding
428 revealed by super-resolution microscopy in which binding became increasingly associated
429 with highly granular multi-glucan surface exposures in response to caspofungin treatments
430 [87].

431 Using multiple approaches, we provide evidence that individual mannan-recognising CTLs
432 recognise different mannan structures that are displayed in distinct binding patterns. CRD4-7-
433 Fc (MR) and hDC-SIGN-Fc recognised α -1,6-mannose backbone with oligomeric α -1,2, α -1,3,
434 and β -1,2-mannan branches while dectin-2-Fc bound Man₉GN₂, which has close similarities
435 to the core *N*-mannan structure in *C. albicans* inner cell wall. Heat-killing and
436 immunofluorescent staining of *C. albicans* cell wall mutants as well as immunogold-labelling
437 and TEM microscopy supported the conclusion that MR and DC-SIGN recognise outer chain
438 *N*-mannan whilst dectin-2 recognises core mannans that are closer to the amide linkage
439 polypeptide of the mannoprotein at the base of the fibrillar layer of the outer cell wall. We
440 observed that CRD4-7-Fc and hDC-SIGN-Fc epitopes were diffusely organised across the
441 plasma membrane plane and within the outer wall mannan fibrils while dectin-2-Fc epitopes
442 were clustered within the inner cell wall in both yeast and hyphal *C. albicans* cells. Clustering
443 of the dectin-2-Fc epitope requires further investigation but may suggest cooperative binding
444 whereby binding of a single dectin-2-Fc could stabilize the target ligand in a way that facilitates
445 bindings of additional PRR molecules. Alternatively certain cell wall proteins that display
446 dectin-2 binding ligands might accumulate in microdomains within the inner cell wall.
447 Membranes of eukaryotic cells are known to organise some proteins into specialised
448 microdomains which compartmentalise cellular processes and serve as organising centres
449 which assemble signalling molecules, facilitate protein and receptor trafficking, vesicular
450 transport and signalling events [88, 89]. Such microdomains have also been described in
451 bacterial membranes and a recently published study suggested that similar microdomains
452 might also exist in fungal cell walls [90]. Therefore, clustered dectin-2-Fc binding could be
453 related to the accumulation of specialised glycosylated proteins at certain parts of the inner
454 cell wall. Nevertheless, these attractive hypothesis should be addressed by future studies.

455 In conclusion, we have demonstrated that mannan epitopes are differentially distributed in the
456 inner and outer layers of fungal cell wall in a clustered or diffuse manner. Immune reactivity of
457 fungal cell surfaces was not correlated with relatedness of the fungal species, and mannan-

458 detecting receptor-probes discriminated between cell surface components generated by the
459 same fungus growing under different conditions. Moreover, individual mannan-recognising
460 CTL probes conferred specificity for distinct mannan epitopes. These findings indicate that the
461 fungal cell wall structures are highly structured but dynamic, and that immune recognition is
462 likely to involve PRRs acting alone and in concert to mount effective immune responses. This
463 type of CTL ligand variation carries significant impact on the design of future fungal
464 diagnostics, vaccine and therapeutics.

465

466 **Materials and Methods**

467 **Expression and purification of Fc conjugated C-type Lectin Receptor proteins**

468 HEK293T cells stably expressing murine dectin-1-Fc and dectin-2-Fc fusion proteins were
469 cultured as described previously [36, 37]. Briefly, cells were cultured in T175 flasks and
470 supernatants were collected. Zeocin (0.4 mg/ml) (Thermo Scientific) was used for selection of
471 cells expressing Fc conjugated proteins. Large scale transient transfections for murine CRD4-
472 7-Fc and CR-Fc were carried out using 100 µg of total plasmid DNA and 100 ml of suspension
473 cultured Expi293F cells (Life Technologies). Supernatants were harvested at day 6. Fc
474 conjugated protein concentrations in supernatants were quantified by ELISA. ELISA plates
475 (Thermofisher) were coated with 100 µl of supernatants and incubated overnight at 4°C. Plates
476 were washed with PBS + Tween 20 (0.05 %) and blocked with 200 µl of 10 % FCS in 1 X PBS
477 for 2 h. Plates were washed with 1 X PBS + Tween 20 (0.05 %) and 100 µl of secondary anti-
478 human antibody conjugated to HRP (Jackson ImmunoResearch) diluted 1/10000 in PBS was
479 added and incubated at room temperature (RT) for 1 h. Wells were washed with 1 X PBS +
480 Tween 20 (0.05 %) and 100 µ of TMB (Thermofisher) were added to develop. Reaction was
481 stopped with 50 µl 2N H₂SO₄ and plates were assayed on a spectrophotometer at 450_{nm} with
482 the necessary λ correction at 570_{nm}. Fc chimeric proteins were purified via affinity based Fast
483 Protein Liquid chromatography using Prosep® Ultra resin (Millipore). Fc conjugated proteins

484 were eluted with 0.1 M glycine (pH 2.5) before neutralisation with 1 M Tris buffer (pH 8) and
485 then dialysed in 1 X PBS overnight. Fc conjugated protein concentration was quantified using
486 NanoVue Spectrophotometer (GE Healthcare).

487 **QC of purified Fc-lectins**

488 Purified proteins were checked via SDS-PAGE gel analysis using 4-12 % Bis-Tris SDS-PAGE
489 gels under reducing conditions (S Fig. 1). ELISA was carried out for confirmation of binding to
490 original target using ELISA protocol described above (S Fig. 1). ELISA plates were coated
491 with live *C. albicans* yeast cells, 25 µg/ml *S. cerevisiae* mannan (SIGMA), 100 µg/ml
492 *C. albicans* yeast β-glucan or PBS overnight (S Fig. 1). Fc chimeric proteins were added at 5
493 µg/ml and serial doubling dilutions were performed to confirm concentration-dependent
494 binding.

495 **Comparison of fungal strains under different parameters**

496 For comparison of fixed and heat-killed *C. albicans* (CAI4-Clp10) cells, a single colony was
497 inoculated into 10 ml YPD (1% yeast extract, 2% glucose, 2% peptone) and incubated
498 overnight at 30°C, 200 rpm. Overnight culture was washed in 1 X PBS and 2.5×10^6 cells
499 were either fixed with 4 % paraformaldehyde or kept at 65°C in a heat block for 2 h prior to
500 staining. For comparison of *C. albicans* (CAI4-Clp10) culture overtime, OD₆₀₀ of overnight
501 culture was measured and culture was diluted to OD₆₀₀ of 0.1 in 50 ml YPD in 250 ml flasks.
502 Cells were collected at OD₆₀₀ 0.2, 0.4, 0.6, 1 and 18, washed in 1 X PBS, fixed with 4 %
503 paraformaldehyde at RT for 45 min, washed and then stained. For comparison of different
504 *C. albicans* isolates and cell wall mutants, cells were fixed at OD₆₀₀ ~ 0.5 prior to staining (S
505 Table 1). For comparison of different *Candida* species and *S. cerevisiae*, cells were fixed in
506 stationary phase, OD₆₀₀ ~ 18 (S Table 1). Samples were stained as described below and
507 analysed on BD Fortessa flow cytometer or in 3D on an UltraVIEW® VoX spinning disk
508 confocal microscope. Three independent biological replicates were performed per sample.

509 **Conditions for generating different morphologies of *C. albicans***

510 Single colonies of *C. albicans* were inoculated into 10 ml YPD and incubated overnight at
511 30°C, 200 rpm. To induce hypha formation, cultures were diluted 1:1333 in milliQ water and
512 then adhered on a poly-L-lysine coated glass slide (Thermo Scientific, Menzel-Gläser) for 30
513 min prior to incubation in pre-warmed RPMI + 10 % FCS at 37°C for 45 min- 3 h 15 min
514 depending on the tested parameter. Slides were then washed in DPBS and fixed with 4 %
515 paraformaldehyde. *C. albicans* pseudohyphae were produced using published conditions with
516 modifications [91]. Overnight culture was collected by centrifugation, washed twice with 0.15
517 M NaCl, resuspended in 0.15 M NaCl and incubated at room temperature for 24 h to induce
518 starvation. After 24 h, cells were transferred into RPMI 1640 at a concentration of 1×10^6 and
519 incubated at 30°C 200rpm for 6 h prior to fixation with 4 % paraformaldehyde. Fixed cells were
520 stained and imaged as described below. To induce goliath cell formation, a single colony of
521 *C. albicans* was inoculated in 4 ml SD media (2% glucose, 6.7g/L yeast nitrogen base without
522 amino acids) and incubated for 24 h at 30°C 200 rpm [62]. Following incubation, 600 µl of
523 culture were washed in three times milliQ water and resuspended in 600 µl milliQ water prior
524 to OD₆₀₀ measurement. To elicit zinc starvation, and hence goliath cell formation, washed cells
525 were inoculated into 4 ml of Limited Zinc Medium (LZM) at OD₆₀₀ 0.2. LZM culture was
526 incubated for 3 days prior to fixation with 4% paraformaldehyde and staining [62].

527 **Immunofluorescent staining of Fc-lectins binding to fungal cells**

528 Yeast cells were counted using an Improved Neubauer haemocytometer and 2.5×10^6 cells
529 were transferred into V-bottomed 96-well tissue culture plates. Plates were centrifuged at 4000
530 rpm 5 min and supernatants were removed. Samples of 1 µg/ml dectin-1-Fc in PBS, 1 % (v/v)
531 FCS or 2 µg/ml of dectin-2-Fc, CRD4-7-Fc, CR-Fc or DC-SIGN-Fc (Thermofisher) in binding
532 buffer (BB) (150 mM NaCl, 10 mM Tris pH 7.4, 10 mM CaCl₂ in sterile water + 1% FCS) were
533 then added to appropriate wells and incubated for 45 min on ice. Cells were washed once in
534 PBS + 1% FCS for dectin-1-Fc or BB buffer for dectin-2-Fc, CRD4-7-Fc, CR-Fc and DC-
535 SIGN-Fc and then stained with Alexa Fluor® 488 goat anti-human IgG antibody (Life

536 Technologies) diluted 1/200 in PBS + 1% FCS or BB buffer and incubated 30 min on ice.
537 Stained cells were washed twice before final resuspension in PBS + 1% FCS or BB buffer.
538 For staining filamentous cells, Fc protein in PBS + 1% FCS or BB buffer at the same
539 concentration as above was added on top of poly-L-lysine slides. Samples were analysed
540 using a BD Fortessa flow cytometer where 10000 events were recorded for each sample from
541 three independent experiments. Median fluorescence intensity for asymmetric peaks and
542 mean fluorescence intensity for symmetric peaks was calculated for each sample using
543 FlowJo v.10 software. Alternatively, 5 µl of yeast cells were added on a poly-L-lysine coated
544 glass slides (Thermo Scientific, Menzel-Gläser) prior to imaging in 3D on an UltraVIEW® VoX
545 spinning disk confocal microscope (Nikon, Surrey, UK).

546 **High Pressure Freezing (HPF) of samples for immunogold labelling of *C. albicans* with**
547 **Fc-lectins for Transmission Electron Microscopy (TEM)**

548 Yeast and hyphal *C. albicans* samples were prepared using high-pressure freezing by
549 EMPACT2 high-pressure freezer and rapid transport system (Leica Microsystems Ltd., Milton
550 Keynes, United Kingdom). Cells were freeze-substituted in 1% acetone (w/v) OsO₄ by using
551 a Leica EMASF2 prior to embedding in Spurr's resin and polymerizing at 60°C for 48 h.
552 Ultrathin sections were cut using a Diatome diamond knife on a Leica UC6 ultramicrotome
553 and sections were mounted onto formvar coated copper grids. Subsequently, sections on
554 formvar coated copper grids were blocked in blocking buffer (PBS + 1% (w/v) BSA and 0.5%
555 (v/v) Tween20) for 20 min prior to incubation in three washes in binding buffer (150 mM NaCl,
556 10 mM Tris pH 7.4, 10 mM CaCl₂ in sterile water, 1% FCS) for 5 min. Sections were then
557 incubated with Fc chimeric proteins (5 µg/ml for yeast and 10 µg/ml for hyphae) for 90 min
558 before six washes in binding buffer for 5 min. Fc protein binding was detected by incubation
559 with Protein A conjugated to 10 nm gold (Aurion) (diluted 1:40 in PBS + 0.1% (w/v) BSA) for
560 60 min prior to six 5 min washes in PBS + 0.1% (w/v) BSA followed by three, 5 min washes in
561 PBS, and three, 5 min washes in water. Sections were stained with uranyl acetate for 1 min

562 prior to three 2 min washes in water and were left to dry. TEM images were taken using a
563 JEM-1400 Plus using an AMT UltraVUE camera.

564 **Glycan microarray analyses of Fc-lectins**

565 The binding specificities of the Fc-lectin receptors were analysed using two types of
566 carbohydrate microarrays: (1) a microarray designated 'Fungal and Bacterial Polysaccharide
567 Array' featuring 19 saccharides (polysaccharides or glycoproteins) and one lipid-linked
568 neoglycolipid (NGL) derived from the chitin hexasaccharide (S Table 2); and (2) a screening
569 microarray of 474 sequence-defined lipid-linked glycan probes, of mammalian and non-
570 mammalian type (S Table 3 B) essentially as previously described [92]; these probes are a
571 subset of a recently generated large screening microarray containing around 900 glycan
572 probes (in-house designation "Array Sets 42-56", which will be published in detail elsewhere).

573 The Fc-lectin binding was performed in both types of arrays essentially as described [28]. In
574 brief, after blocking the slides with 0.02% v/v Casein (Pierce) and 1% BSA (Sigma) diluted in
575 HBS (10 mM HEPES-buffered saline, pH 7.4, 150 mM NaCl) with 10 mM CaCl₂, the
576 microarrays were overlaid with the Fc-lectins precomplexed with the biotinylated goat anti-
577 human IgG (Vector) for 2 hours. The Fc-lectin-antibody complexes were prepared by
578 preincubating the –Fc-lectin with the antibody at equimolar ratios for 1 hour, followed by
579 dilution in the blocking solution to give the final Fc-lectin concentration: dectin-2-Fc 10 µg/ml,
580 CRD4-7-Fc 20 µg/ml and hDC-SIGN-Fc 2 µg/ml. Dectin-1-Fc used as control for the Fungal
581 and Bacterial Array was analysed non-precomplexed at 20 µg/ml in the blocking solution 0.5%
582 v/v casein (Pierce) in HBS. The binding was detected with Alexa Fluor-647-labeled
583 streptavidin (Molecular Probes, 1 µg/ml). All steps were carried out at ambient temperature.
584 Details of the glycan library including the sources of saccharides, the generation of the
585 microarrays, imaging, and data analysis are in the Supplementary glycan microarray
586 document (S Table 4) in accordance with the Minimum Information Required for A Glycomics
587 Experiment (MIRAGE) guidelines for reporting glycan microarray-based data [93].

588 **Acknowledgements**

589 We thank Luisa Martinez-Pomares and Darryl Jackson from Nottingham University for
590 providing CRD4-7-Fc and CR-Fc plasmids; Fiona M. Rudkin for advice on protein expression
591 and purification; Louise Walker for high pressure freezing of samples for TEM analysis; David
592 Williams for *C. albicans* purified mannan and β -glucan preparations; Dhara Malavia for
593 providing *C. albicans* goliath cells, the University of Aberdeen Core Microscopy & Histology
594 Facility (Kevin MacKenzie, Lucinda Wight, Debbie Wilkinson), Iain Fraser Cytometry Centre
595 (Raif Yuecel). The neoglycolipid-based glycan microarrays contain several saccharides
596 provided by collaborators whom we thank as well as members of the Glycosciences
597 Laboratory for their collaboration in the establishment of the microarray system.

598

599 **Author Contributions**

600 IV, JAW, GDB & NARG conceived and designed the experiments; IV, LMS, MHTS, ASP
601 performed experiments; IV, JAW, LMS, ASP, YL & NARG analysed data and NARG, GDB,
602 WC & TF contributed reagents / materials/ analysis tools: IV, LMS, ASP & NARG wrote the
603 paper and all authors revised and commented on the manuscript.

604 **Funding:** This work was supported by the Wellcome Trust Investigator, Collaborative,
605 Equipment, Strategic and Biomedical Resource awards (086827, 075470, 097377, 101873,
606 200208, 093378 and 099197), the Applied Molecular Biosciences Unit-UCIBIO (FCT/MCTES
607 UID/Multi/04378/2019), and by the MRC Centre for Medical Mycology (N006364/1). The
608 University of Aberdeen funded a studentship to IV as part of NARG's Wellcome Senior
609 Investigator Award.

610 **Competing interests:** The authors have declared no conflict of interests.

611

612

613 References

- 614 1. Low CY, Rotstein C. Emerging fungal infections in immunocompromised patients.
615 F1000 medicine reports. 2011;3:14-. doi: 10.3410/M3-14. PubMed PMID: 21876720.
- 616 2. Kim J, Sudbery P. *Candida albicans*, a major human fungal pathogen. The Journal of
617 Microbiology. 2011;49(2):171. doi: 10.1007/s12275-011-1064-7.
- 618 3. Enoch DA, Ludlam HA, Brown NM. Invasive fungal infections: a review of
619 epidemiology and management options. Journal of Medical Microbiology. 2006;55(7):809-
620 18. doi: doi:10.1099/jmm.0.46548-0.
- 621 4. Deng Z, Kiyuna A, Hasegawa M, Nakasone I, Hosokawa A, Suzuki M. Oral
622 candidiasis in patients receiving radiation therapy for head and neck cancer.
623 Otolaryngology–Head and Neck Surgery. 2010;143(2):242-7. doi:
624 10.1016/j.otohns.2010.02.003.
- 625 5. Armstrong-James D, Meintjes G, Brown GD. A neglected epidemic: fungal infections
626 in HIV/AIDS. Trends in Microbiology. 2014;22(3):120-7. doi:
627 <https://doi.org/10.1016/j.tim.2014.01.001>.
- 628 6. Rajasingham R, Smith RM, Park BJ, Jarvis JN, Govender NP, Chiller TM, et al.
629 Global burden of disease of HIV-associated cryptococcal meningitis: an updated analysis.
630 The Lancet Infectious Diseases. 2017;17(8):873-81. doi: [https://doi.org/10.1016/S1473-
631 3099\(17\)30243-8](https://doi.org/10.1016/S1473-3099(17)30243-8).
- 632 7. Brown GD. Innate Antifungal Immunity: The Key Role of Phagocytes. Annual Review
633 of Immunology. 2011;29(1):1-21. doi: 10.1146/annurev-immunol-030409-101229.
- 634 8. Becker KL, Ifrim DC, Quintin J, Netea MG, van de Veerdonk FL. Antifungal innate
635 immunity: recognition and inflammatory networks. Seminars in Immunopathology.
636 2015;37(2):107-16. doi: 10.1007/s00281-014-0467-z.
- 637 9. Erwig LP, Gow NAR. Interactions of fungal pathogens with phagocytes. Nature
638 Reviews Microbiology. 2016;14:163. doi: 10.1038/nrmicro.2015.21.
- 639 10. Miramón P, Kasper L, Hube B. Thriving within the host: *Candida* spp. interactions
640 with phagocytic cells. Medical Microbiology and Immunology. 2013;202(3):183-95. doi:
641 10.1007/s00430-013-0288-z.
- 642 11. Netea MG, Joosten LAB, van der Meer JWM, Kullberg B-J, van de Veerdonk FL.
643 Immune defence against *Candida* fungal infections. Nature Reviews Immunology.
644 2015;15:630. doi: 10.1038/nri3897.
- 645 12. Gow NAR, Netea MG. Medical mycology and fungal immunology: new research
646 perspectives addressing a major world health challenge. Philosophical transactions of the
647 Royal Society of London Series B, Biological sciences. 2016;371(1709):20150462. doi:
648 10.1098/rstb.2015.0462. PubMed PMID: 28080988.
- 649 13. Netea MG, Gow NAR, Munro CA, Bates S, Collins C, Ferwerda G, et al. Immune
650 sensing of *Candida albicans* requires cooperative recognition of mannans and glucans by
651 lectin and Toll-like receptors. The Journal of Clinical Investigation. 2006;116(6):1642-50. doi:
652 10.1172/JCI27114.
- 653 14. Latgé J-P. The cell wall: a carbohydrate armour for the fungal cell. Molecular
654 Microbiology. 2007;66(2):279-90. doi: 10.1111/j.1365-2958.2007.05872.x.
- 655 15. Gow NAR, Latge J-P, Munro CA. The Fungal Cell Wall: Structure, Biosynthesis, and
656 Function. Microbiology Spectrum. 2017;5(3). doi: doi:10.1128/microbiolspec.FUNK-0035-
657 2016.
- 658 16. Bowman SM, Free SJ. The structure and synthesis of the fungal cell wall. BioEssays.
659 2006;28(8):799-808. doi: 10.1002/bies.20441.
- 660 17. Gow NAR, Hube B. Importance of the *Candida albicans* cell wall during
661 commensalism and infection. Current Opinion in Microbiology. 2012;15(4):406-12. doi:
662 <https://doi.org/10.1016/j.mib.2012.04.005>.
- 663 18. Hall RA, Gow NAR. Mannosylation in *Candida albicans*: role in cell wall function and
664 immune recognition. Molecular Microbiology. 2013;90(6):1147-61. doi: 10.1111/mmi.12426.

- 665 19. Kędzierska A, Kochan P, Pietrzyk A, Kędzierska J. Current status of fungal cell wall
666 components in the immunodiagnosics of invasive fungal infections in humans:
667 galactomannan, mannan and (1→3)-β-D-glucan antigens. *European Journal of Clinical*
668 *Microbiology & Infectious Diseases*. 2007;26(11):755-66. doi: 10.1007/s10096-007-0373-6.
- 669 20. Komarova BS, Wong SSW, Orekhova MV, Tsvetkov YE, Krylov VB, Beauvais A, et
670 al. Chemical Synthesis and Application of Biotinylated Oligo-α-(1 → 3)-d-Glucosides To
671 Study the Antibody and Cytokine Response against the Cell Wall α-(1 → 3)-d-Glucan of
672 *Aspergillus fumigatus*. *The Journal of Organic Chemistry*. 2018;83(21):12965-76. doi:
673 10.1021/acs.joc.8b01142.
- 674 21. Krylov VB, Solovev AS, Argunov DA, Latgé JP, Nifantiev NE. Reinvestigation of
675 carbohydrate specificity of EB-A2 monoclonal antibody used in the immune detection of
676 *Aspergillus fumigatus* galactomannan. *Heliyon*. 2019;5(1):e01173-e. doi:
677 10.1016/j.heliyon.2019.e01173. PubMed PMID: 30766929.
- 678 22. Ene IV, Adya AK, Wehmeier S, Brand AC, MacCallum DM, Gow NAR, et al. Host
679 carbon sources modulate cell wall architecture, drug resistance and virulence in a fungal
680 pathogen. *Cellular Microbiology*. 2012;14(9):1319-35. doi: 10.1111/j.1462-
681 5822.2012.01813.x.
- 682 23. Lewis LE, Bain JM, Lowes C, Gillespie C, Rudkin FM, Gow NAR, et al. Stage specific
683 assessment of *Candida albicans* phagocytosis by macrophages identifies cell wall
684 composition and morphogenesis as key determinants. *PLoS pathogens*.
685 2012;8(3):e1002578-e. doi: 10.1371/journal.ppat.1002578. PubMed PMID: 22438806.
- 686 24. Lowman DW, Greene RR, Bearden DW, Kruppa MD, Pottier M, Monteiro MA, et al.
687 Novel structural features in *Candida albicans* hyphal glucan provide a basis for differential
688 innate immune recognition of hyphae versus yeast. *The Journal of biological chemistry*.
689 2014;289(6):3432-43. Epub 12/16. doi: 10.1074/jbc.M113.529131. PubMed PMID:
690 24344127.
- 691 25. Ballou ER, Avelar GM, Childers DS, Mackie J, Bain JM, Wagener J, et al. Lactate
692 signalling regulates fungal β-glucan masking and immune evasion. *Nature microbiology*.
693 2016;2:16238-. doi: 10.1038/nmicrobiol.2016.238. PubMed PMID: 27941860.
- 694 26. Luo G, Ibrahim AS, Spellberg B, Nobile CJ, Mitchell AP, Fu Y. *Candida albicans*
695 *Hyr1p* confers resistance to neutrophil killing and is a potential vaccine target. *The Journal of*
696 *infectious diseases*. 2010;201(11):1718-28. doi: 10.1086/652407. PubMed PMID: 20415594.
- 697 27. Sousa MdG, Reid DM, Schweighoffer E, Tybulewicz V, Ruland J, Langhorne J, et al.
698 Restoration of pattern recognition receptor costimulation to treat chromoblastomycosis, a
699 chronic fungal infection of the skin. *Cell host & microbe*. 2011;9(5):436-43. doi:
700 10.1016/j.chom.2011.04.005. PubMed PMID: 21575914.
- 701 28. Rudkin FM, Raziunaite I, Workman H, Essono S, Belmonte R, MacCallum DM, et al.
702 Single human B cell-derived monoclonal anti-*Candida* antibodies enhance phagocytosis and
703 protect against disseminated candidiasis. *Nature Communications*. 2018;9(1):5288. doi:
704 10.1038/s41467-018-07738-1.
- 705 29. Zelensky AN, Gready JE. The C-type lectin-like domain superfamily. *The FEBS*
706 *Journal*. 2005;272(24):6179-217. doi: 10.1111/j.1742-4658.2005.05031.x.
- 707 30. Kerrigan AM, Brown GD. C-type lectins and phagocytosis. *Immunobiology*.
708 2009;214(7):562-75. doi: 10.1016/j.imbio.2008.11.003. PubMed PMID: 19261355.
- 709 31. Kerrigan AM, Brown GD. Syk-coupled C-type lectins in immunity. *Trends in*
710 *Immunology*. 2011;32(4):151-6. doi: <https://doi.org/10.1016/j.it.2011.01.002>.
- 711 32. Dambuza IM, Brown GD. C-type lectins in immunity: recent developments. *Current*
712 *Opinion in Immunology*. 2015;32:21-7. doi: <https://doi.org/10.1016/j.coi.2014.12.002>.
- 713 33. Tang J, Lin G, Langdon WY, Tao L, Zhang J. Regulation of C-Type Lectin Receptor-
714 Mediated Antifungal Immunity. *Frontiers in immunology*. 2018;9:123-. doi:
715 10.3389/fimmu.2018.00123. PubMed PMID: 29449845.
- 716 34. Taylor ME, Drickamer K. Structural requirements for high affinity binding of complex
717 ligands by the macrophage mannose receptor. *Journal of Biological Chemistry*.
718 1993;268(1):399-404.

- 719 35. Ariizumi K, Shen G-L, Shikano S, Xu S, Ritter R, Kumamoto T, et al. Identification of
720 a Novel, Dendritic Cell-associated Molecule, Dectin-1, by Subtractive cDNA Cloning. *Journal*
721 *of Biological Chemistry*. 2000;275(26):20157-67. doi: 10.1074/jbc.M909512199.
- 722 36. Graham LM, Tsoni SV, Willment JA, Williams DL, Taylor PR, Gordon S, et al. Soluble
723 Dectin-1 as a tool to detect β -glucans. *Journal of Immunological Methods*. 2006;314(1):164-
724 9. doi: <https://doi.org/10.1016/j.jim.2006.05.013>.
- 725 37. McGreal EP, Brown GD, Martinez-Pomares L, Rosas M, Taylor PR, Gordon S, et al.
726 The carbohydrate-recognition domain of Dectin-2 is a C-type lectin with specificity for high
727 mannose. *Glycobiology*. 2006;16(5):422-30. doi: 10.1093/glycob/cwj077.
- 728 38. Cambi A, Netea MG, Mora-Montes HM, Gow NAR, Hato SV, Lowman DW, et al.
729 Dendritic Cell Interaction with *Candida albicans* Critically Depends on N-Linked Mannan.
730 *Journal of Biological Chemistry*. 2008;283(29):20590-9. doi: 10.1074/jbc.M709334200.
- 731 39. Stappers MHT, Clark AE, Aimanianda V, Bidula S, Reid DM, Asamaphan P, et al.
732 Recognition of DHN-melanin by a C-type lectin receptor is required for immunity to
733 *Aspergillus*. *Nature*. 2018;555:382. doi: 10.1038/nature25974
734 <https://www.nature.com/articles/nature25974#supplementary-information>.
- 735 40. Stahl PD, Ezekowitz RAB. The mannose receptor is a pattern recognition receptor
736 involved in host defense. *Current Opinion in Immunology*. 1998;10(1):50-5. doi:
737 [https://doi.org/10.1016/S0952-7915\(98\)80031-9](https://doi.org/10.1016/S0952-7915(98)80031-9).
- 738 41. J Smits G, C Kapteyn J, van den Ende H, M Klis F. Cell wall dynamics in yeast.
739 *Current Opinion in Microbiology*. 1999;2(4):348-52. doi: [https://doi.org/10.1016/S1369-5274\(99\)80061-7](https://doi.org/10.1016/S1369-5274(99)80061-7).
- 740 42. Brown GD, Gordon S. A new receptor for β -glucans. *Nature*. 2001;413:36. doi:
741 10.1038/35092620.
- 742 43. Domer JE. *Candida* Cell Wall Mannan: A Polysaccharide with Diverse Immunologic
743 Properties. *Critical Reviews in Microbiology*. 1989;17(1):33-51. doi:
744 10.3109/10408418909105721.
- 745 44. Shibata N, Suzuki A, Kobayashi H, Okawa Y. Chemical structure of the cell-wall
746 mannan of *Candida albicans* serotype A and its difference in yeast and hyphal forms. *The*
747 *Biochemical journal*. 2007;404(3):365-72. Epub 05/29. doi: 10.1042/BJ20070081. PubMed
748 PMID: 17331070.
- 749 45. Tada H, Nemoto E, Shimauchi H, Watanabe T, Mikami T, Matsumoto T, et al.
750 *Saccharomyces cerevisiae*- and *Candida albicans*-Derived Mannan Induced Production of
751 Tumor Necrosis Factor Alpha by Human Monocytes in a CD14- and Toll-Like Receptor 4-
752 Dependent Manner. *Microbiology and Immunology*. 2002;46(7):503-12. doi: 10.1111/j.1348-
753 0421.2002.tb02727.x.
- 754 46. Poulain D, Trinel P-A, Iбата-Ombetta S, Jouault T, Sacchetti P, Lefebvre P, et al.
755 *Candida albicans* Phospholipomannan Is Sensed through Toll-Like Receptors. *The Journal*
756 *of Infectious Diseases*. 2003;188(1):165-72. doi: 10.1086/375784.
- 757 47. Cambi A, Gijzen K, de Vries IJM, Torensma R, Joosten B, Adema GJ, et al. The C-
758 type lectin DC-SIGN (CD209) is an antigen-uptake receptor for *Candida albicans* on
759 dendritic cells. *European Journal of Immunology*. 2003;33(2):532-8. doi:
760 10.1002/immu.200310029.
- 761 48. Kohatsu L, Hsu DK, Jegalian AG, Liu F-T, Baum LG. Galectin-3 Induces Death of
762 *Candida* Species Expressing Specific β -1,2-Linked Mannans. *The Journal of Immunology*.
763 2006;177(7):4718-26. doi: 10.4049/jimmunol.177.7.4718.
- 764 49. Sato K, Yang X-I, Yudate T, Chung J-S, Wu J, Luby-Phelps K, et al. Dectin-2 Is a
765 Pattern Recognition Receptor for Fungi That Couples with the Fc Receptor γ Chain to
766 Induce Innate Immune Responses. *Journal of Biological Chemistry*. 2006;281(50):38854-66.
767 doi: 10.1074/jbc.M606542200.
- 768 50. Yamasaki S, Matsumoto M, Takeuchi O, Matsuzawa T, Ishikawa E, Sakuma M, et al.
769 C-type lectin Mincle is an activating receptor for pathogenic fungus, *Malassezia*.
770 *Proceedings of the National Academy of Sciences of the United States of America*.
771

- 772 2009;106(6):1897-902. Epub 01/26. doi: 10.1073/pnas.0805177106. PubMed PMID:
773 19171887.
- 774 51. Kullberg BJ, Verschuere I, van der Meer JWM, Joosten LAB, Netea MG, Gow NAR.
775 Variable recognition of *Candida albicans* strains by TLR4 and lectin recognition receptors.
776 Medical Mycology. 2010;48(7):897-903. doi: 10.3109/13693781003621575.
- 777 52. Zhu L-L, Zhao X-Q, Jiang C, You Y, Chen X-P, Jiang Y-Y, et al. C-Type Lectin
778 Receptors Dectin-3 and Dectin-2 Form a Heterodimeric Pattern-Recognition Receptor for
779 Host Defense against Fungal Infection. Immunity. 2013;39(2):324-34. doi:
780 <https://doi.org/10.1016/j.immuni.2013.05.017>.
- 781 53. Lionakis MS, Levitz SM. Host Control of Fungal Infections: Lessons from Basic
782 Studies and Human Cohorts. Annual Review of Immunology. 2018;36(1):157-91. doi:
783 10.1146/annurev-immunol-042617-053318.
- 784 54. Guo Y, Chang Q, Cheng L, Xiong S, Jia X, Lin X, et al. C-Type Lectin Receptor
785 CD23 Is Required for Host Defense against *Candida albicans* and *Aspergillus fumigatus*
786 Infection. The Journal of Immunology. 2018;201(8):2427. doi: 10.4049/jimmunol.1800620.
- 787 55. Linehan SA, Martínez-Pomares L, Silva RPD, Gordon S. Endogenous ligands of
788 carbohydrate recognition domains of the mannose receptor in murine macrophages,
789 endothelial cells and secretory cells; potential relevance to inflammation and immunity.
790 European Journal of Immunology. 2001;31(6):1857-66. doi: 10.1002/1521-
791 4141(200106)31:6<1857::AID-IMMU1857>3.0.CO;2-D.
- 792 56. Martínez-Pomares L, Kosco-Vilbois M, Darley E, Tree P, Herren S, Bonnefoy JY, et
793 al. Fc chimeric protein containing the cysteine-rich domain of the murine mannose receptor
794 binds to macrophages from splenic marginal zone and lymph node subcapsular sinus and to
795 germinal centers. The Journal of experimental medicine. 1996;184(5):1927-37. PubMed
796 PMID: 8920880.
- 797 57. Leteux C, Chai W, Loveless RW, Yuen CT, Uhlin-Hansen L, Combarrous Y, et al.
798 The cysteine-rich domain of the macrophage mannose receptor is a multispecific lectin that
799 recognizes chondroitin sulfates A and B and sulfated oligosaccharides of blood group
800 Lewis(a) and Lewis(x) types in addition to the sulfated N-glycans of lutropin. The Journal of
801 experimental medicine. 2000;191(7):1117-26. doi: 10.1084/jem.191.7.1117. PubMed PMID:
802 10748230.
- 803 58. Glittenberg MT, Silas S, MacCallum DM, Gow NAR, Ligoxygakis P. Wild-type
804 *Drosophila melanogaster* as an alternative model system for investigating the pathogenicity
805 of *Candida albicans*. Disease Models & Mechanisms. 2011;4(4):504-14. doi:
806 10.1242/dmm.006619.
- 807 59. MacCallum DM, Castillo L, Nather K, Munro CA, Brown AJP, Gow NAR, et al.
808 Property differences among the four major *Candida albicans* strain clades. Eukaryotic cell.
809 2009;8(3):373-87. Epub 01/16. doi: 10.1128/EC.00387-08. PubMed PMID: 19151328.
- 810 60. Brand A, MacCallum DM, Brown AJP, Gow NAR, Odds FC. Ectopic expression of
811 URA3 can influence the virulence phenotypes and proteome of *Candida albicans* but can be
812 overcome by targeted reintegration of URA3 at the RPS10 locus. Eukaryotic cell.
813 2004;3(4):900-9. doi: 10.1128/EC.3.4.900-909.2004. PubMed PMID: 15302823.
- 814 61. Wheeler RT, Kombe D, Agarwala SD, Fink GR. Dynamic, Morphotype-Specific
815 *Candida albicans* β -Glucan Exposure during Infection and Drug Treatment. PLOS
816 Pathogens. 2008;4(12):e1000227. doi: 10.1371/journal.ppat.1000227.
- 817 62. Malavia D, Lehtovirta-Morley LE, Alamir O, Weiß E, Gow NAR, Hube B, et al. Zinc
818 Limitation Induces a Hyper-Adherent Goliath Phenotype in *Candida albicans*. Frontiers in
819 Microbiology. 2017;8(2238). doi: 10.3389/fmicb.2017.02238.
- 820 63. Gantner BN, Simmons RM, Underhill DM. Dectin-1 mediates macrophage
821 recognition of *Candida albicans* yeast but not filaments. The EMBO journal.
822 2005;24(6):1277-86. Epub 02/24. doi: 10.1038/sj.emboj.7600594. PubMed PMID:
823 15729357.
- 824 64. Palma AS, Feizi T, Zhang Y, Stoll MS, Lawson AM, Díaz-Rodríguez E, et al. Ligands
825 for the β -Glucan Receptor, Dectin-1, Assigned Using "Designer" Microarrays of

- 826 Oligosaccharide Probes (Neoglycolipids) Generated from Glucan Polysaccharides. *Journal of Biological Chemistry*. 2006;281(9):5771-9. doi: 10.1074/jbc.M511461200.
- 827
- 828 65. Hobson RP, Munro CA, Bates S, MacCallum DM, Cutler JE, Heinsbroek SEM, et al.
- 829 Loss of Cell Wall Mannosylphosphate in *Candida albicans* Does Not Influence Macrophage
- 830 Recognition. *Journal of Biological Chemistry*. 2004;279(38):39628-35. doi:
- 831 10.1074/jbc.M405003200.
- 832 66. Hall RA, Bates S, Lenardon MD, Maccallum DM, Wagener J, Lowman DW, et al. The
- 833 Mnn2 mannosyltransferase family modulates mannoprotein fibril length, immune recognition
- 834 and virulence of *Candida albicans*. *PLoS pathogens*. 2013;9(4):e1003276-e. doi:
- 835 10.1371/journal.ppat.1003276. PubMed PMID: 23633946.
- 836 67. Bates S, Hughes HB, Munro CA, Thomas WPH, MacCallum DM, Bertram G, et al.
- 837 Outer Chain *N*-Glycans Are Required for Cell Wall Integrity and Virulence of *Candida*
- 838 *albicans*. *Journal of Biological Chemistry*. 2006;281(1):90-8. doi: 10.1074/jbc.M510360200.
- 839 68. Bates S, MacCallum DM, Bertram G, Munro CA, Hughes HB, Buurman ET, et al.
- 840 *Candida albicans* Pmr1p, a Secretory Pathway P-type Ca²⁺/Mn²⁺-ATPase, Is Required for
- 841 Glycosylation and Virulence. *Journal of Biological Chemistry*. 2005;280(24):23408-15. doi:
- 842 10.1074/jbc.M502162200.
- 843 69. Feinberg H, Jégouzo SAF, Rex MJ, Drickamer K, Weis WI, Taylor ME. Mechanism of
- 844 pathogen recognition by human dectin-2. *The Journal of biological chemistry*.
- 845 2017;292(32):13402-14. Epub 06/26. doi: 10.1074/jbc.M117.799080. PubMed PMID:
- 846 28652405.
- 847 70. Palma AS, Liu Y, Zhang H, Zhang Y, McCleary BV, Yu G, et al. Unravelling glucan
- 848 recognition systems by glycome microarrays using the designer approach and mass
- 849 spectrometry. *Molecular & cellular proteomics : MCP*. 2015;14(4):974-88. Epub 02/10. doi:
- 850 10.1074/mcp.M115.048272. PubMed PMID: 25670804.
- 851 71. Zhang H, Palma AS, Zhang Y, Childs RA, Liu Y, Mitchell DA, et al. Generation and
- 852 characterization of β 1,2-gluco-oligosaccharide probes from *Brucella abortus* cyclic β -glucan
- 853 and their recognition by C-type lectins of the immune system. *Glycobiology*.
- 854 2016;26(10):1086-96. Epub 10/18. doi: 10.1093/glycob/cww041. PubMed PMID: 27053576.
- 855 72. Kang BK, Schlesinger LS. Characterization of mannose receptor-dependent
- 856 phagocytosis mediated by *Mycobacterium tuberculosis* lipoarabinomannan. *Infection and*
- 857 *immunity*. 1998;66(6):2769-77. PubMed PMID: 9596746.
- 858 73. van Liempt E, Bank CMC, Mehta P, Garcí a-Vallejo JJ, Kwar ZS, Geyer R, et al.
- 859 Specificity of DC-SIGN for mannose- and fucose-containing glycans. *FEBS Letters*.
- 860 2006;580(26):6123-31. doi: 10.1016/j.febslet.2006.10.009.
- 861 74. Gow NAR, van de Veerdonk FL, Brown AJP, Netea MG. *Candida albicans*
- 862 morphogenesis and host defence: discriminating invasion from colonization. *Nature Reviews*
- 863 *Microbiology*. 2011;10:112. doi: 10.1038/nrmicro2711.
- 864 75. Grumaz C, Lorenz S, Stevens P, Lindemann E, Schöck U, Retey J, et al. Species
- 865 and condition specific adaptation of the transcriptional landscapes in *Candida albicans* and
- 866 *Candida dubliniensis*. *BMC genomics*. 2013;14:212-. doi: 10.1186/1471-2164-14-212.
- 867 PubMed PMID: 23547856.
- 868 76. Marakalala MJ, Vautier S, Potrykus J, Walker LA, Shepardson KM, Hopke A, et al.
- 869 Differential adaptation of *Candida albicans* in vivo modulates immune recognition by dectin-
- 870 1. *PLoS pathogens*. 2013;9(4):e1003315-e. doi: 10.1371/journal.ppat.1003315. PubMed
- 871 PMID: 23637604.
- 872 77. Phan QT, Belanger PH, Filler SG. Role of hyphal formation in interactions of *Candida*
- 873 *albicans* with endothelial cells. *Infection and immunity*. 2000;68(6):3485-90. PubMed PMID:
- 874 10816502.
- 875 78. McKenzie CGJ, Koser U, Lewis LE, Bain JM, Mora-Montes HM, Barker RN, et al.
- 876 Contribution of *Candida albicans* Cell Wall Components to Recognition by and Escape from
- 877 Murine Macrophages. *Infection and Immunity*. 2010;78(4):1650-8. doi: 10.1128/iai.00001-10.
- 878 79. Wächter B, Wilson D, Haedicke K, Dalle F, Hube B. From Attachment to Damage:
- 879 Defined Genes of *Candida albicans* Mediate Adhesion, Invasion and Damage during

- 880 Interaction with Oral Epithelial Cells. PLOS ONE. 2011;6(2):e17046. doi:
881 10.1371/journal.pone.0017046.
- 882 80. Bain JM, Louw J, Lewis LE, Okai B, Walls CA, Ballou ER, et al. *Candida albicans*
883 Hypha Formation and Mannan Masking of β -Glucan Inhibit Macrophage Phagosome
884 Maturation. mBio. 2014;5(6):e01874-14. doi: 10.1128/mBio.01874-14.
- 885 81. Moyes DL, Wilson D, Richardson JP, Mogavero S, Tang SX, Wernecke J, et al.
886 Candidalysin is a fungal peptide toxin critical for mucosal infection. Nature.
887 2016;532(7597):64-8. Epub 03/30. doi: 10.1038/nature17625. PubMed PMID: 27027296.
- 888 82. Lee SJ, Zheng N-Y, Clavijo M, Nussenzweig MC. Normal Host Defense during
889 Systemic Candidiasis in Mannose Receptor-Deficient Mice. Infection and Immunity.
890 2003;71(1):437. doi: 10.1128/IAI.71.1.437-445.2003.
- 891 83. Sudbery P, Gow N, Berman J. The distinct morphogenic states of *Candida albicans*.
892 Trends in Microbiology. 2004;12(7):317-24. doi: <https://doi.org/10.1016/j.tim.2004.05.008>.
- 893 84. da Silva Dantas A, Lee KK, Raziunaite I, Schaefer K, Wagener J, Yadav B, et al. Cell
894 biology of *Candida albicans*-host interactions. Current opinion in microbiology. 2016;34:111-
895 8. doi: 10.1016/j.mib.2016.08.006. PubMed PMID: 27689902.
- 896 85. Gow NAR, Yadav B. Microbe Profile: *Candida albicans*: a shape-changing,
897 opportunistic pathogenic fungus of humans. Microbiology. 2017;163(8):1145-7. doi:
898 doi:10.1099/mic.0.000499.
- 899 86. Mukaremera L, Lee KK, Mora-Montes HM, Gow NAR. *Candida albicans* Yeast,
900 Pseudohyphal, and Hyphal Morphogenesis Differentially Affects Immune Recognition.
901 Frontiers in Immunology. 2017;8(629). doi: 10.3389/fimmu.2017.00629.
- 902 87. Lin J, Wester MJ, Graus MS, Lidke KA, Neumann AK. Nanoscopic cell-wall
903 architecture of an immunogenic ligand in *Candida albicans* during antifungal drug treatment.
904 Molecular biology of the cell. 2016;27(6):1002-14. doi: 10.1091/mbc.E15-06-0355. PubMed
905 PMID: 26792838.
- 906 88. Maxfield FR. Plasma membrane microdomains. Current Opinion in Cell Biology.
907 2002;14(4):483-7. doi: [https://doi.org/10.1016/S0955-0674\(02\)00351-4](https://doi.org/10.1016/S0955-0674(02)00351-4).
- 908 89. Laude AJ, Prior IA. Plasma membrane microdomains: organization, function and
909 trafficking. Molecular membrane biology. 2004;21(3):193-205. doi:
910 10.1080/09687680410001700517. PubMed PMID: 15204627.
- 911 90. Lipke PN, Klotz SA, Dufrene YF, Jackson DN, Garcia-Sherman MC. Amyloid-Like β -
912 Aggregates as Force-Sensitive Switches in Fungal Biofilms and Infections. Microbiology and
913 molecular biology reviews : MMBR. 2017;82(1):e00035-17. doi: 10.1128/MMBR.00035-17.
914 PubMed PMID: 29187516.
- 915 91. Merson-Davies LA, Odds FC. A Morphology Index for Characterization of Cell Shape
916 in *Candida albicans*. Microbiology. 1989;135(11):3143-52. doi: doi:10.1099/00221287-135-
917 11-3143.
- 918 92. Palma AS, Liu Y, Childs RA, Herbert C, Wang D, Chai W, et al. The human epithelial
919 carcinoma antigen recognized by monoclonal antibody AE3 is expressed on a sulfoglycolipid
920 in addition to neoplastic mucins. Biochem Biophys Res Commun. 2011;408(4):548-52. Epub
921 04/19. doi: 10.1016/j.bbrc.2011.04.055. PubMed PMID: 21527252.
- 922 93. Liu Y, McBride R, Stoll M, Palma AS, Silva L, Agravat S, et al. The minimum
923 information required for a glycomics experiment (MIRAGE) project: improving the standards
924 for reporting glycan microarray-based data. Glycobiology. 2016;27(4):280-4. doi:
925 10.1093/glycob/cww118.
- 926 94. Tavanti A, Davidson AD, Gow NAR, Maiden MCJ, Odds FC. *Candida orthopsilosis*
927 and *Candida metapsilosis* spp. nov. to replace *Candida parapsilosis* groups II and III.
928 Journal of clinical microbiology. 2005;43(1):284-92. doi: 10.1128/JCM.43.1.284-292.2005.
929 PubMed PMID: 15634984.

930

931

932

933 **Figure Legends**

934 **Figure 1. Binding of CTL receptors does not correlate with fungal phylogenetic**
935 **relationships.** (A) Fc-lectin binding to different *Candida* species and *S. cerevisiae* displayed
936 according to phylogenetic relationships in agreement with the published dendrogram [94] and
937 represented as Median Fluorescence Intensity (MFI) of probe binding. (B) Representative
938 images of FACS histograms. (C) Comparison of Fc-lectin binding pattern to evolutionary
939 closely related *C. albicans* and *C. dubliniensis* yeast cells. For immunofluorescence staining
940 and flow cytometry experiments, 2.5×10^6 cells were used in each analysis. Data were
941 obtained using a BD Fortessa flow cytometer and median fluorescence values were used for
942 quantification of probe binding. 3D visualisation on an UltraView® VoX spinning disk confocal
943 microscope was also used to observe binding patterns of Fc-lectins on the cell surfaces.
944 Represented data are means \pm SEM, n=3. Scale bars represent 4 μ m.

945

946 **Figure 2. Binding of Fc-lectin probes to different *C. albicans* isolates.** (A) Binding of Fc-
947 lectin probes to the laboratory control strain (CAI4-CIp10), and to virulent (SC5314, Ysu751,
948 J990102) and attenuated (IHEM3742, AM2003/0609, HUN92) clinical isolates. Binding to
949 yeast cells is represented as Median Fluorescent Intensities (MFI). (B) Indirect
950 immunofluorescence staining of hyphae of virulent *C. albicans* (SC5314, J990102) and
951 attenuated (IHEM3742, HUN92) isolates with Fc-lectin probes. For immunofluorescence
952 staining and flow cytometry experiments, 2.5×10^6 cells were used per analysis. Data were
953 obtained using a BD Fortessa flow cytometer and 3D visualisation on an UltraView® VoX
954 spinning disk confocal microscope was also used to observe Fc-lectin binding patterns.
955 Median fluorescence values were used for quantification and results are represented as
956 means \pm SEM, n=3. Statistical analyses were performed using Kruskal-Wallis with Dunn's
957 post-hoc test. Scale bars represent 4 μ m.

958

959 **Figure 3. Expression of ligands for CTL receptors during the batch growth of**
960 ***C. albicans*.** (A) The OD₆₀₀ values of samples taken for analysis during different growth stages
961 are indicated. (B) Median Fluorescent Intensity (MFI) values from indirect
962 immunofluorescence staining of *C. albicans* (SC5314) yeast cells by dectin-2-Fc, CRD4-7-Fc
963 and dectin-1-Fc. For immunofluorescence staining and flow cytometry experiments, 2.5×10^6
964 cells were used per analysis. Data were obtained using a BD Fortessa flow cytometer and
965 median fluorescence values were used for quantification. Results are represented as means
966 \pm SEM, n=3. Statistical analysis were performed using Kruskal-Wallis with Dunn's post-hoc
967 tests.

968

969 **Figure 4. Indirect immunofluorescence of Fc-lectin binding to target ligands in the**
970 ***C. albicans* cell wall during different stages of hyphal growth.** Representative images of
971 immunofluorescence staining of Fc-lectin binding to *C. albicans* (SC5314) hyphae over
972 prolonged periods of growth by dectin-2-Fc (A), CRD4-7-Fc (B) and dectin-1-Fc (C). Data were
973 obtained using UltraView® VoX confocal spinning disk microscope and scale bars represent
974 4 μ m.

975

976 **Figure 5. Indirect immunofluorescence of Fc-lectin binding to different *C. albicans***
977 **morphological forms.** Representative images of immunofluorescence staining of Fc-lectin
978 binding to *C. albicans* yeast, hyphae, pseudohyphae (SC5314) and goliath (BWP17 + Clp30)
979 cells by dectin-2-Fc (A), CRD4-7-Fc (B), dectin-1-Fc (C) and CR-Fc (D). Data were obtained
980 using UltraView® VoX confocal spinning disk microscope and scale bars represent 4 μ m for
981 yeast and pseudohyphae images and 6 μ m for hyphae.

982

983 **Figure 6. Immunogold localisation of Fc-lectin probes on *C. albicans* yeast and hypha**
984 **cell walls.** Representative TEM images of at least one experiment where Protein A gold
985 conjugate was used to detect dectin-2-Fc (A), CRD4-7-Fc (B) and CR-Fc (C) binding on

986 *C. albicans* (SC5314) cell walls. TEM images were taken using a JEM-1400 Plus using an
987 AMT UltraVUE camera. Scale bars represent 100 nm.

988

989 **Figure 7. Binding of Fc-lectin probes to *C. albicans* fixed and heat-killed yeast cells.**

990 Quantification of Fc-lectin probe binding to WT (live) and HK (heat-killed) cells for dectin-2-Fc
991 (blue) (A), CRD4-7-Fc (red) (B), dectin-1-Fc (green) (C) and CR-Fc (orange) (A-C) binding to
992 WT *C. albicans* yeast cells (dark bars), HK *C. albicans* yeast cells (light bars). Blocking
993 experiments are also shown in which Fc-lectins were preincubated with purified *C. albicans*
994 cell wall mannan (25 µg/ml) or β-glucan (for dectin-1-Fc, 100 µg/ml) and subsequent binding
995 to WT 4% paraformaldehyde fixed *C. albicans* yeast cells (crossed bars). For flow cytometry
996 experiments, 2.5×10^6 cells were used per analysis. Data were obtained using a BD Fortessa
997 flow cytometer and median fluorescence values were used for quantification of probe binding.
998 Data are means ± SEM, n = 3. Statistical analyses with One Way Anova with Tukey's post-
999 hoc test.

1000

1001 **Figure 8. hDC-SIGN-Fc binding across the inner and outer cell wall of *C. albicans*. (A)**

1002 hDC-SIGN-Fc binding to WT 4% paraformaldehyde fixed *C. albicans* (CAI4-Clp10) yeast cells
1003 compared to 65°C HK cells and hDC-SIGN-Fc blocked with *C. albicans* cell wall mannan
1004 (25 µg/ml). (B) Binding of hDC-SIGN-Fc blocked with *C. albicans* cell wall mannan (25 µg/ml)
1005 or *S. cerevisiae* cell wall mannan (25 µg/ml) to WT 4% paraformaldehyde fixed *C. albicans*
1006 yeast cells. (C) Indirect immunofluorescence staining of different *C. albicans* (SC5314,
1007 BWP17 + Clp30 for goliath cells) morphological forms. (D) Immunogold localisation of hDC-
1008 SIGN-Fc on *C. albicans* (SC5314) yeast and hyphae cells. (E) Representative images of
1009 immunofluorescence staining of hDC-SIGN-Fc binding to *C. albicans* (SC5314) hyphae over
1010 prolonged periods of growth. Data were obtained using UltraView® VoX confocal spinning
1011 disk microscope, a BD Fortessa flow cytometer and JEM-1400 Plus using an AMT UltraVUE
1012 camera for TEM images. Scale bars represent 4 µm for immunofluorescence images and 100

1013 nm for TEMs. For immunofluorescence staining and flow cytometry experiments, 2.5×10^6
1014 cells were used per treatment. Median fluorescence values were used for quantification of
1015 hDC-SIGN-Fc binding and represented data are means \pm SEM, $n = 3$. Statistical analyses
1016 used One Way Anova with Tukey's post-hoc test.

1017

1018 **Figure 9. Fc-lectin binding profiles to *C. albicans* cell wall glycosylation mutants.** (A)

1019 Indirect immunofluorescence images of Fc-conjugated CTL probes binding to *C. albicans* O-
1020 mannan and N-mannan cell wall mutants of *C. albicans* (as described in the text). (B) Heat-
1021 map of increased or reduced binding of Fc-lectins to *C. albicans* cell wall mutants relative to
1022 the SC5314 clinical isolate. Dark red (increased binding) to yellow (reduced binding). Data
1023 were obtained using UltraView® VoX confocal spinning disk microscope. Scale bars represent
1024 4 μm .

1025

1026 **Figure 10. Glycan microarray analyses of Fc-lectins using the fungal and bacterial**

1027 **polysaccharides.** Binding signals of CRD4-7-Fc (A), hDC-SIGN-Fc (B) and dectin-1-Fc (C)
1028 to a variety of fungal and bacterial polysaccharides. The saccharide positions and predominant
1029 oligosaccharide sequences are specified in the supplementary materials (S Table 2). The
1030 binding signals are means of the fluorescence intensities of duplicate spots printed at the high
1031 level of probe arrayed 0.1 ng/spot (saccharide positions 1-19) and at 5 fmol/spot (position 20).
1032 The error bars represent half the difference between the two values.

1033

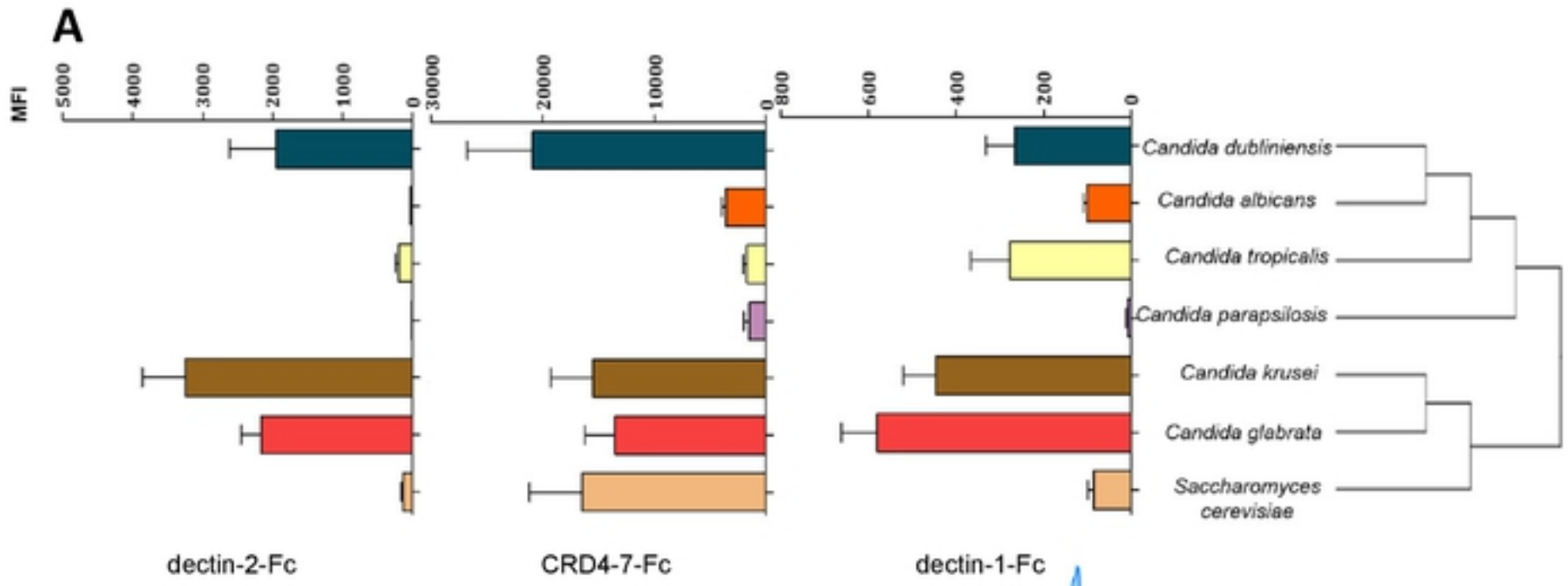
1034 **Figure 11. Microarray analysis of Fc-lectins using a screening array of sequence-**

1035 **defined glycan probes.** Binding signals of dectin-2-Fc (A), CRD4-7-Fc (B) and hDC-SIGN-
1036 Fc (C) to a variety of sequence-defined polysaccharides. The glycan resembling the core N-
1037 mannan structure in *C. albicans* cell wall (position 250) is highlighted in dectin-2-Fc panel. The
1038 binding signals are means of the fluorescence intensities of duplicate spots printed at 5
1039 fmol/probe. The error bars represent half of the difference between the two values. The glycan
1040 probes are grouped according to their backbone-type sequences as annotated by the colored

1041 panels: disaccharide based: lactose (Lac) and *N*-acetyllactosamine (LacNAc); tetrasaccharide
1042 based: lacto-*N*-neo-tetraose (LNnT) and lacto-*N*-tetraose (LNT); poly-*N*-acetyllactosamine
1043 (PolyLacNAc); *N*-glycans; gangliosides; *O*-glycan-related; polysialyl; glycosaminoglycans
1044 (GAGs); homo-oligomers of glucose and of other monosaccharides, and other non-classified
1045 sequences (miscellaneous, Misc). The list of glycan probes and their sequences are in
1046 supplementary materials (S Table 3 B).

1047

1048 **S Figure 1. Concentration response curves of Fc-lectin binding to target antigens via**
1049 **ELISA.** Purified Fc-lectin probes were screened against whole *C. albicans* (SC5314) yeast
1050 cells (black), purified cell wall mannan (green) or purified yeast β -glucan (blue) (A). Fc-lectin
1051 integrity was checked via reducing SDS-Page, expected band sizes were dectin-1-Fc 55 kDa,
1052 dectin-2-Fc 55 kDa, CRD4-7-Fc 110 kDa, CR-Fc 50 kDa, hDC-SIGN-Fc 69kDa (B).



B bioRxiv preprint doi: <https://doi.org/10.1101/677104>; this version posted June 19, 2019. The copyright holder for this preprint (which was not certified by peer review) is the author/funder, who has granted bioRxiv a license to display the preprint in perpetuity. It is made available under aCC-BY 4.0 International license.

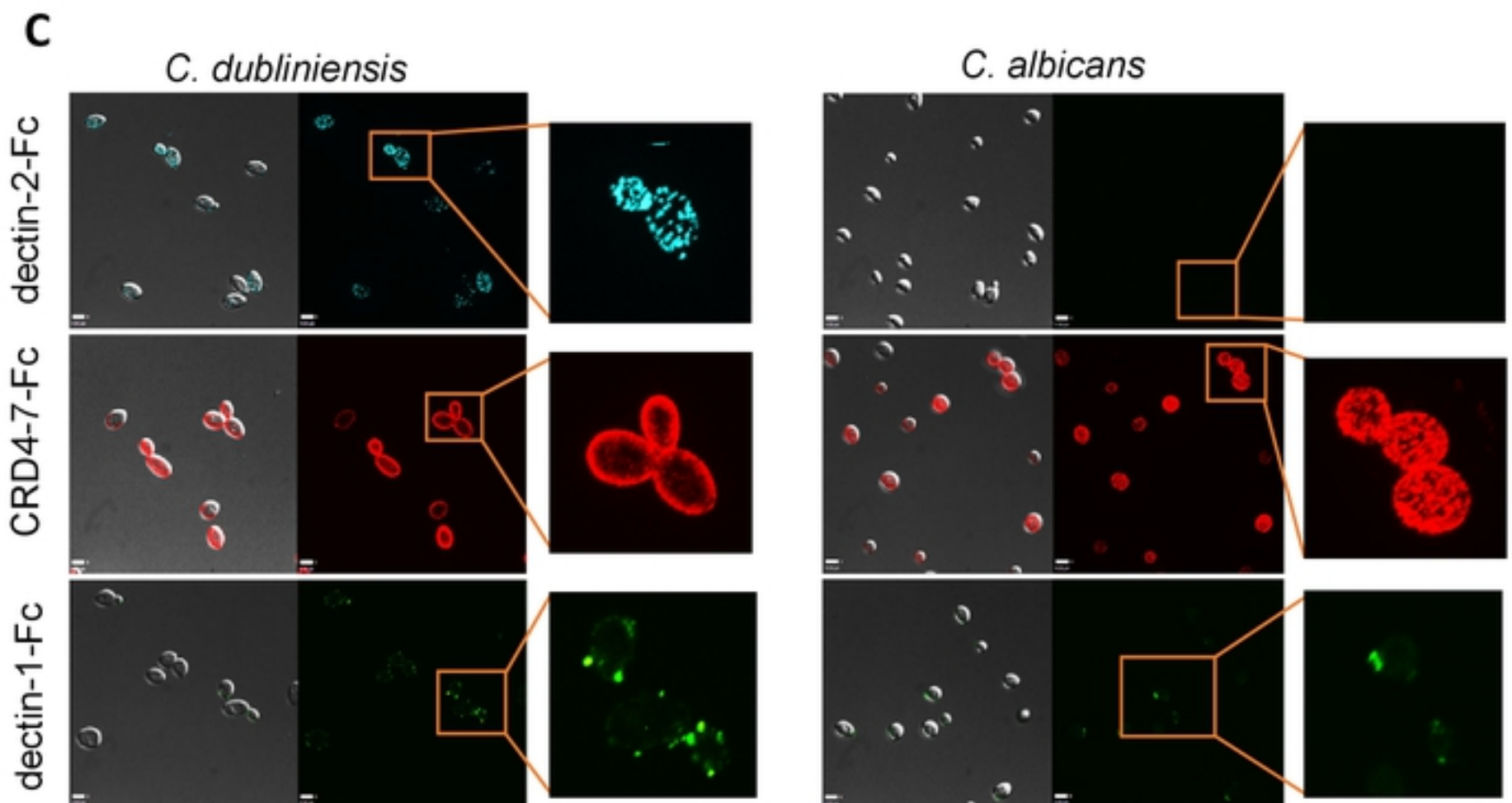
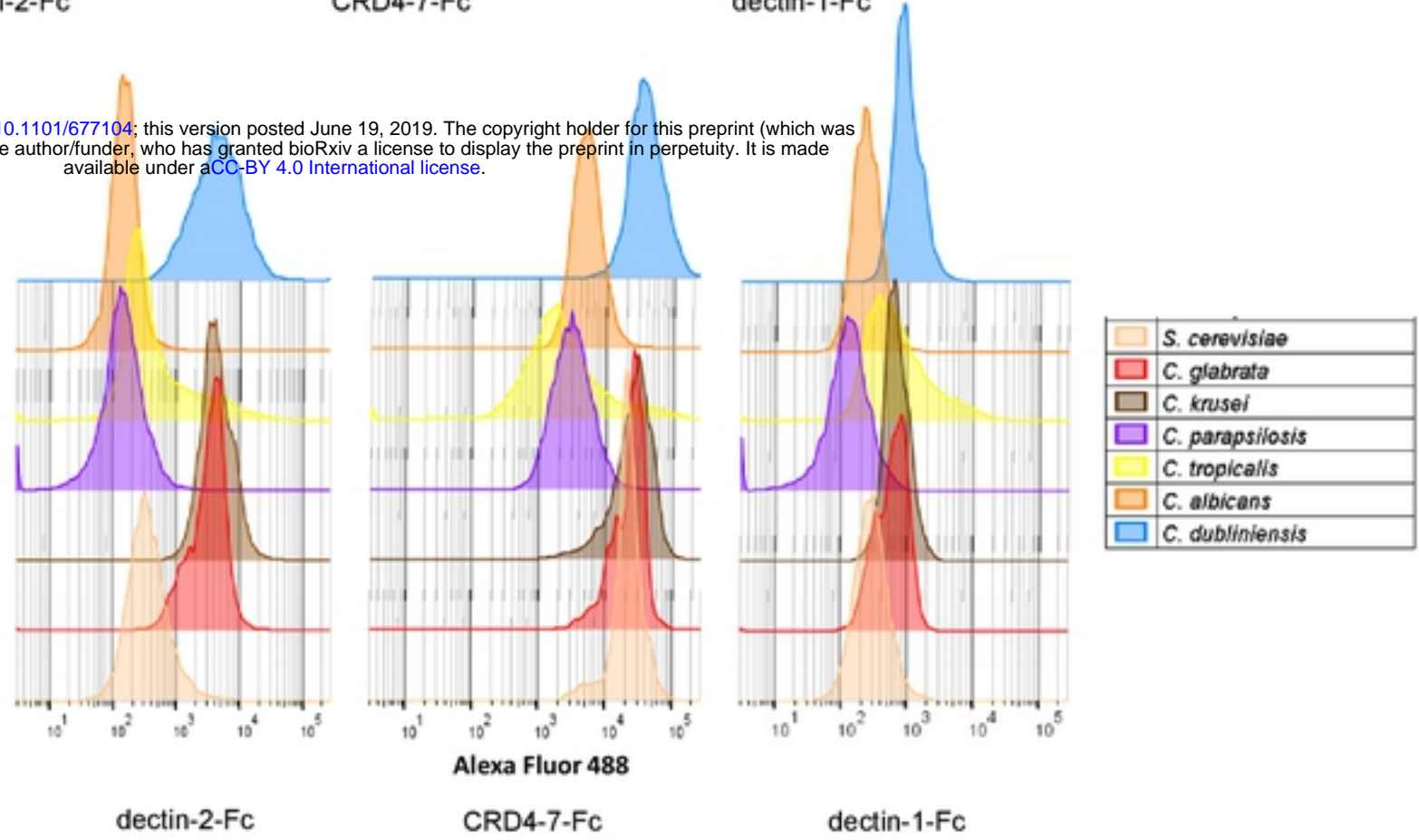
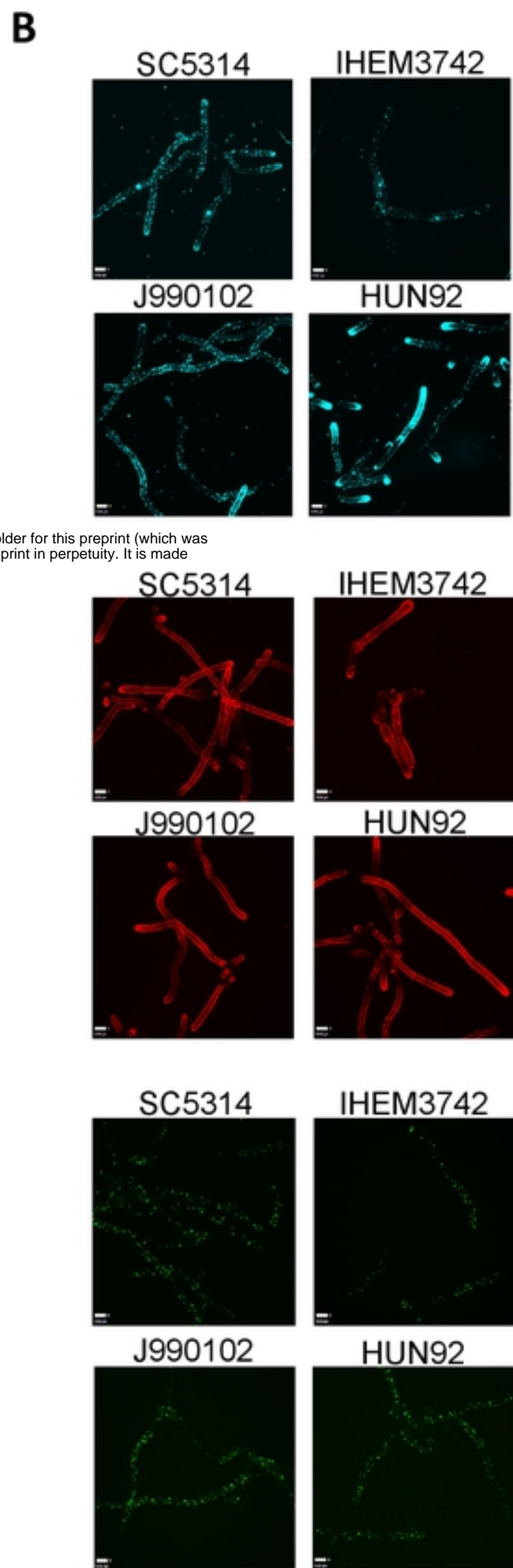
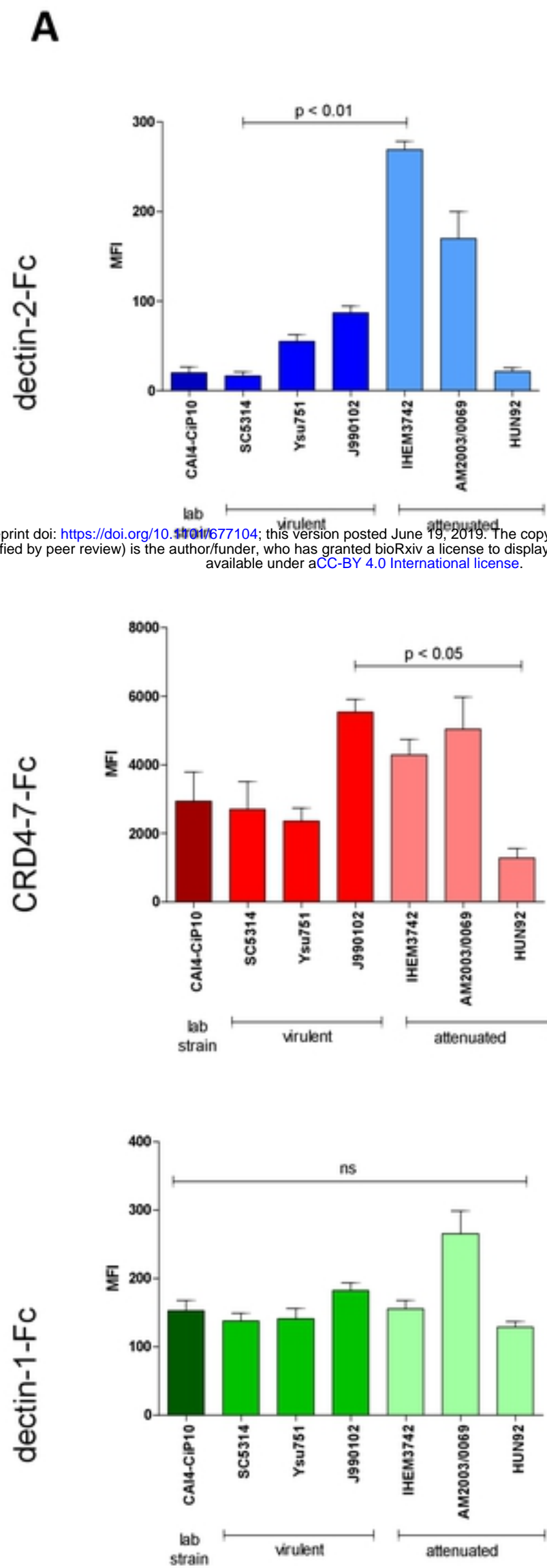
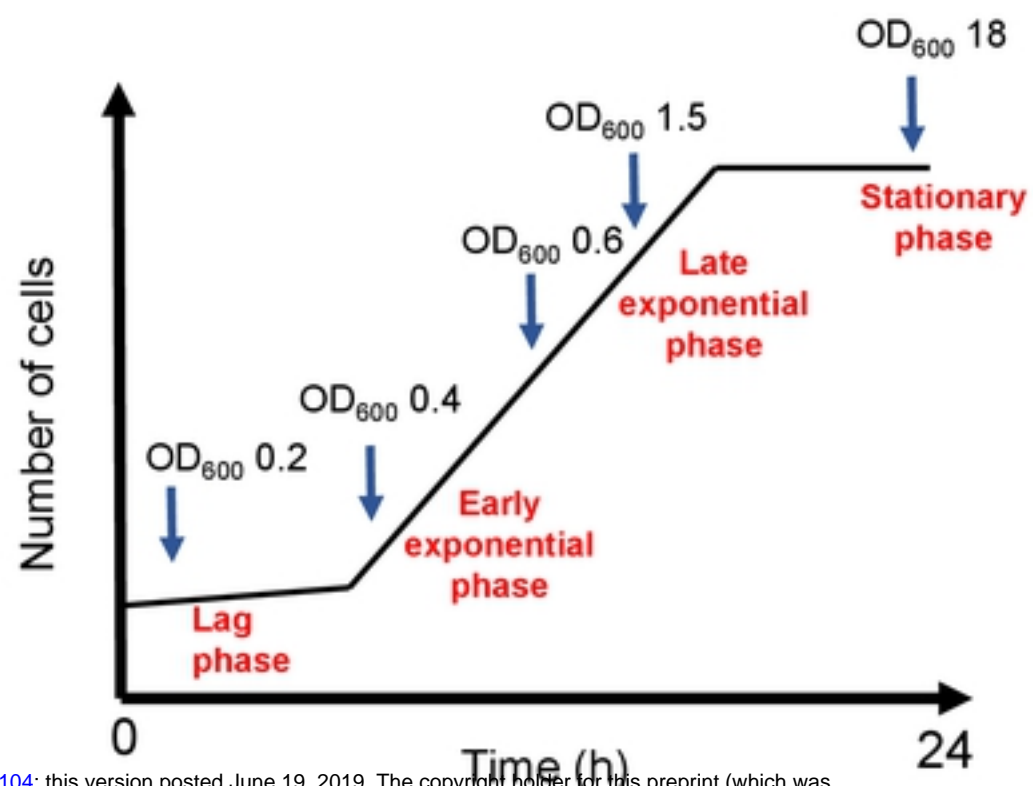


Fig. 1

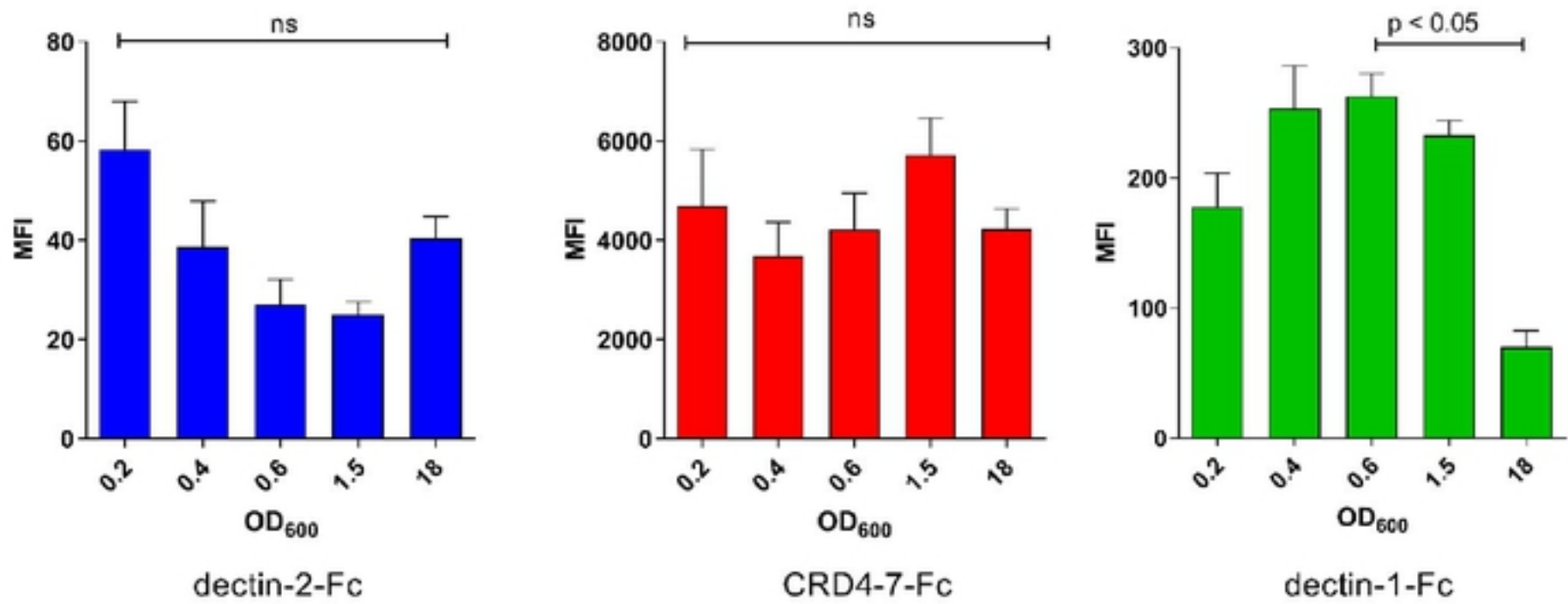


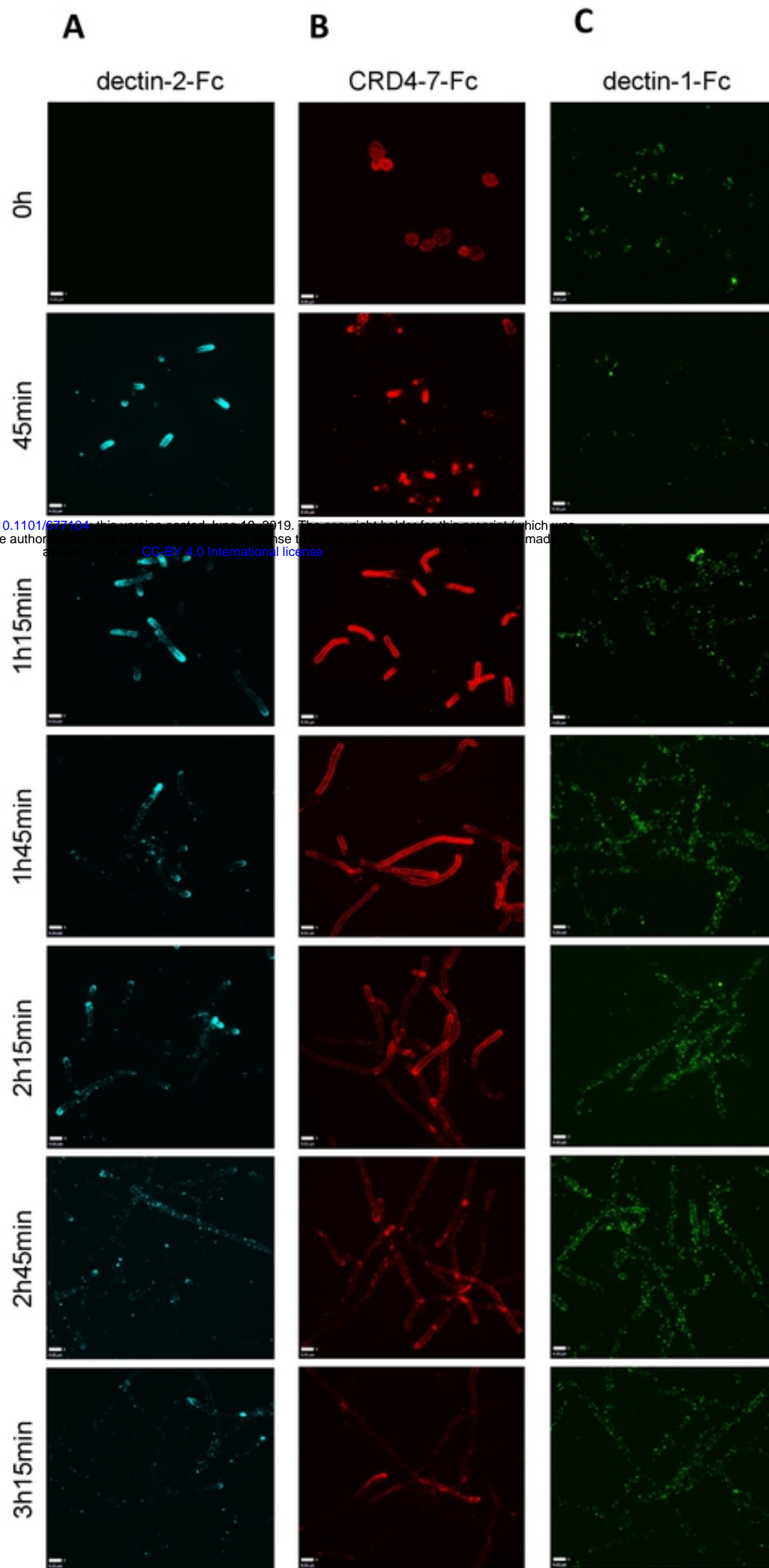
bioRxiv preprint doi: <https://doi.org/10.1101/677104>; this version posted June 19, 2019. The copyright holder for this preprint (which was not certified by peer review) is the author/funder, who has granted bioRxiv a license to display the preprint in perpetuity. It is made available under aCC-BY 4.0 International license.

Fig. 2

A

bioRxiv preprint doi: <https://doi.org/10.1101/677104>; this version posted June 19, 2019. The copyright holder for this preprint (which was not certified by peer review) is the author/funder, who has granted bioRxiv a license to display the preprint in perpetuity. It is made available under aCC-BY 4.0 International license.

B**Fig. 3**



bioRxiv preprint doi: <https://doi.org/10.1101/677104>; this version posted June 10, 2019. The copyright holder for this preprint (which was not certified by peer review) is the author/funder, who has granted bioRxiv a license to display the preprint in perpetuity. It is made available under aCC-BY 4.0 International license.

Fig. 4

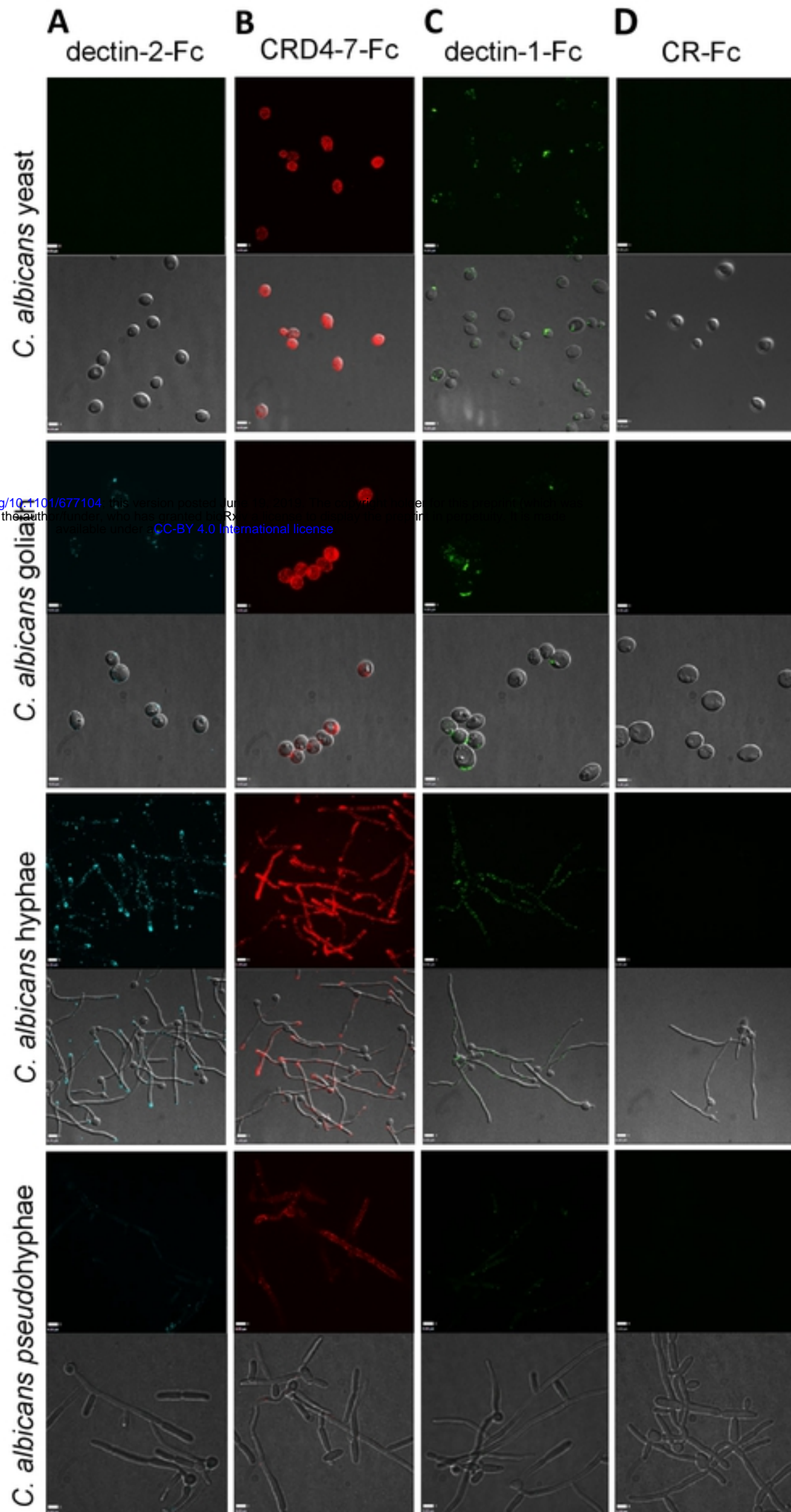
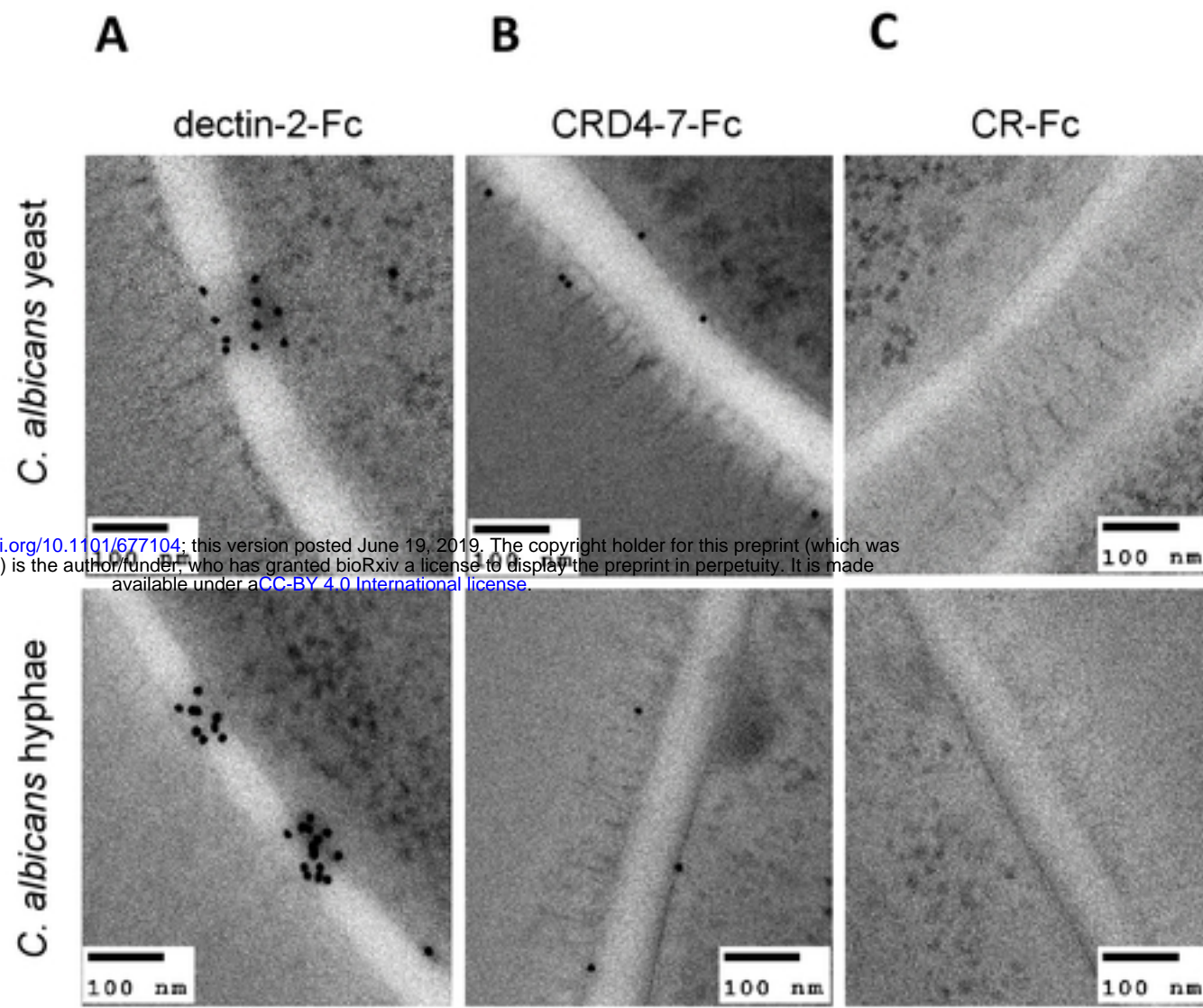


Fig. 5



bioRxiv preprint doi: <https://doi.org/10.1101/677104>; this version posted June 19, 2019. The copyright holder for this preprint (which was not certified by peer review) is the author/funder, who has granted bioRxiv a license to display the preprint in perpetuity. It is made available under aCC-BY 4.0 International license.

Fig. 6

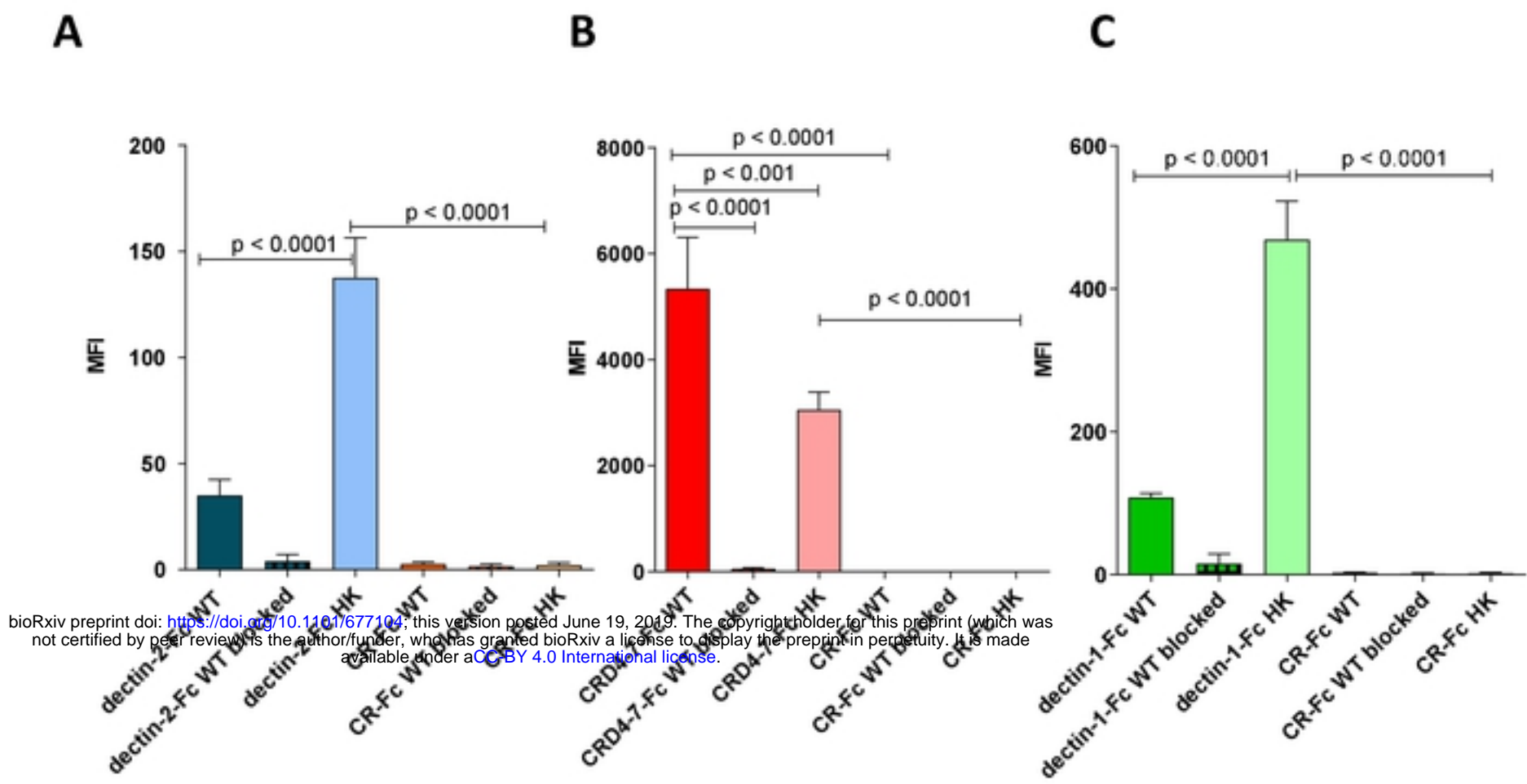
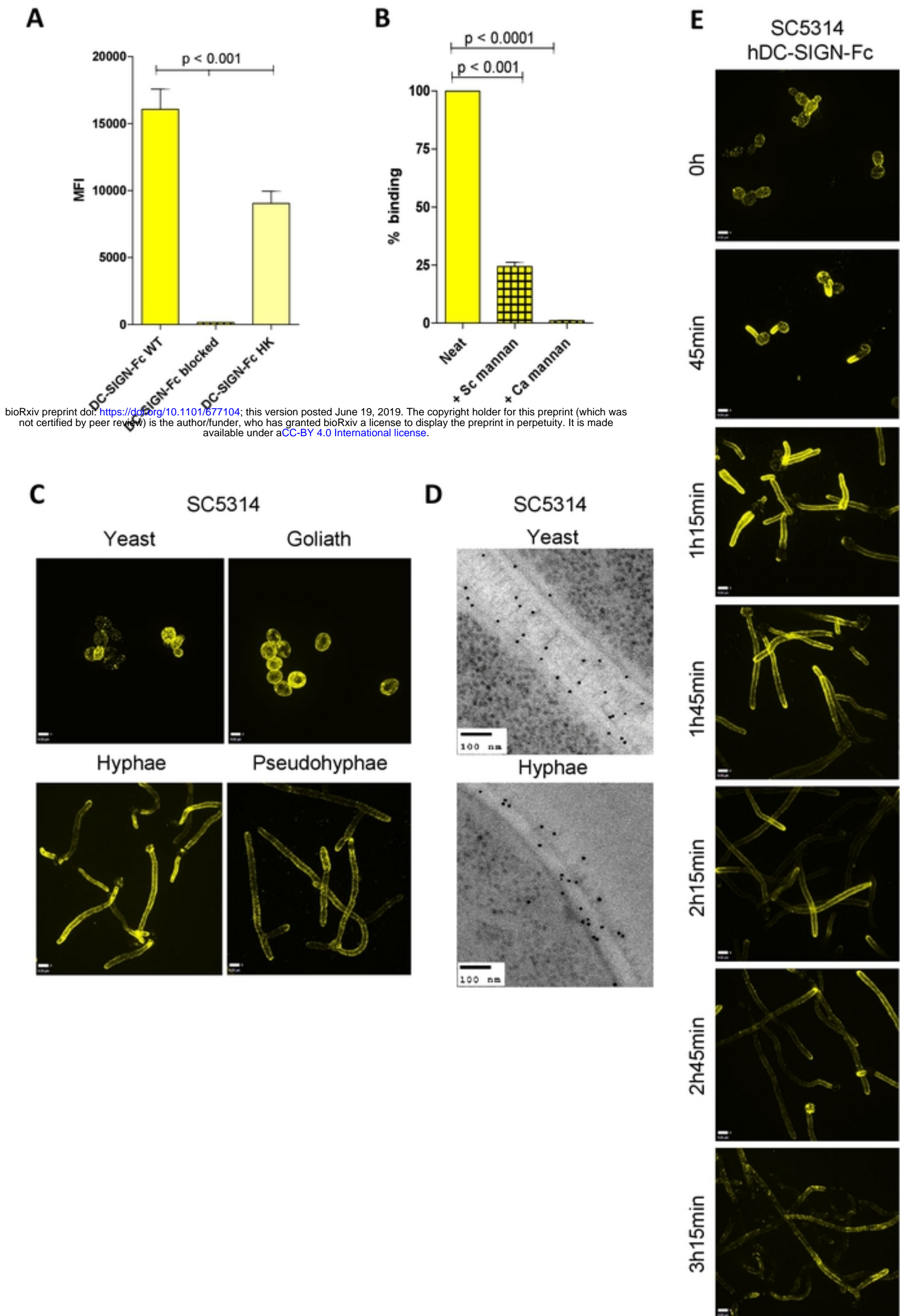
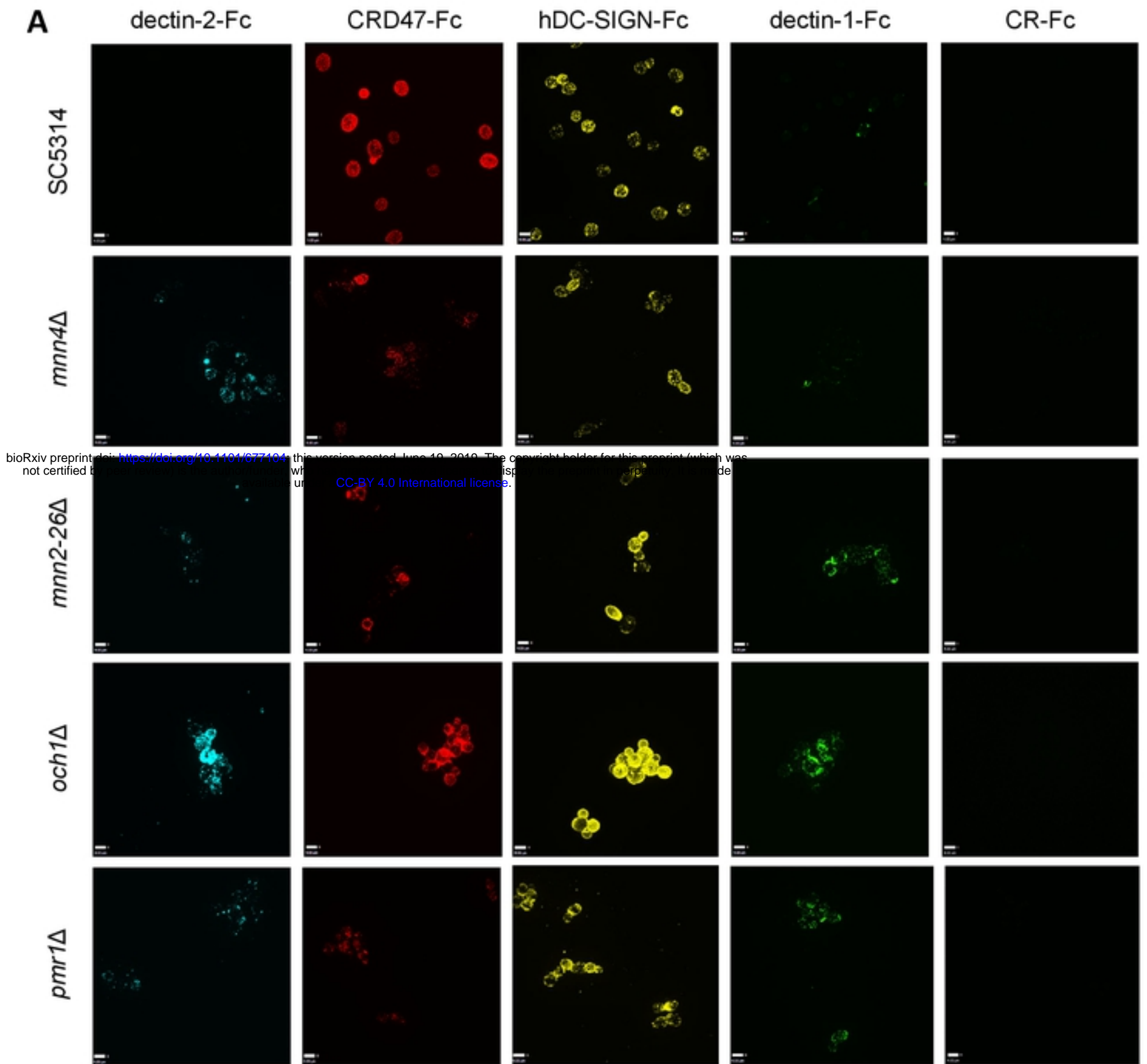


Fig. 7



bioRxiv preprint doi: <https://doi.org/10.1101/677104>; this version posted June 19, 2019. The copyright holder for this preprint (which was not certified by peer review) is the author/funder, who has granted bioRxiv a license to display the preprint in perpetuity. It is made available under aCC-BY 4.0 International license.

Fig. 8



bioRxiv preprint doi: <https://doi.org/10.1101/077104>; this version posted June 10, 2019. The copyright holder for this preprint (which was not certified by peer review) is the author/funder, who has granted bioRxiv a license to display the preprint in perpetuity. It is made available under aCC-BY 4.0 International license.

B

		Mannan			β -glucan	Neg. Control
		dectin-2-Fc	CRD4-7-Fc	hDC-SIGN-Fc	dectin-1-Fc	CR-Fc
N-mannan outer chains	SC5314	Yellow	Red	Red	Yellow	No binding
	<i>mnn4</i> Δ	Red	Yellow	Red	Yellow	
	<i>mnn2-26</i> Δ	Red	Orange	Red	Red	
N- and O-mannan	<i>och1</i> Δ	Red	Red	Red	Red	
	<i>pmr1</i> Δ	Red	Orange	Red	Red	



Fig. 9

bioRxiv preprint doi: <https://doi.org/10.1101/677104>; this version posted June 19, 2019. The copyright holder for this preprint (which was not certified by peer review) is the author/funder, who has granted bioRxiv a license to display the preprint in perpetuity. It is made available under aCC-BY 4.0 International license.

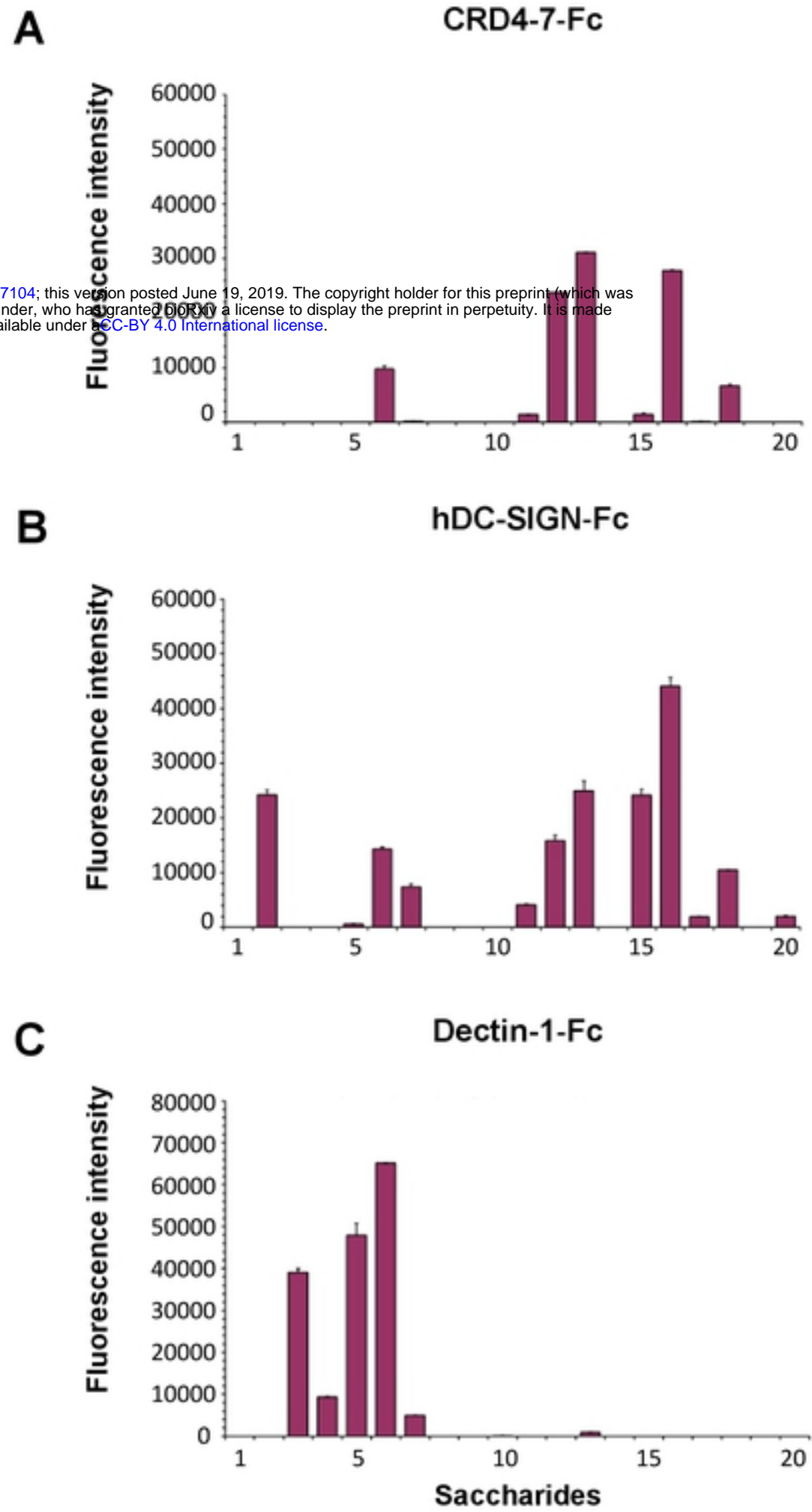
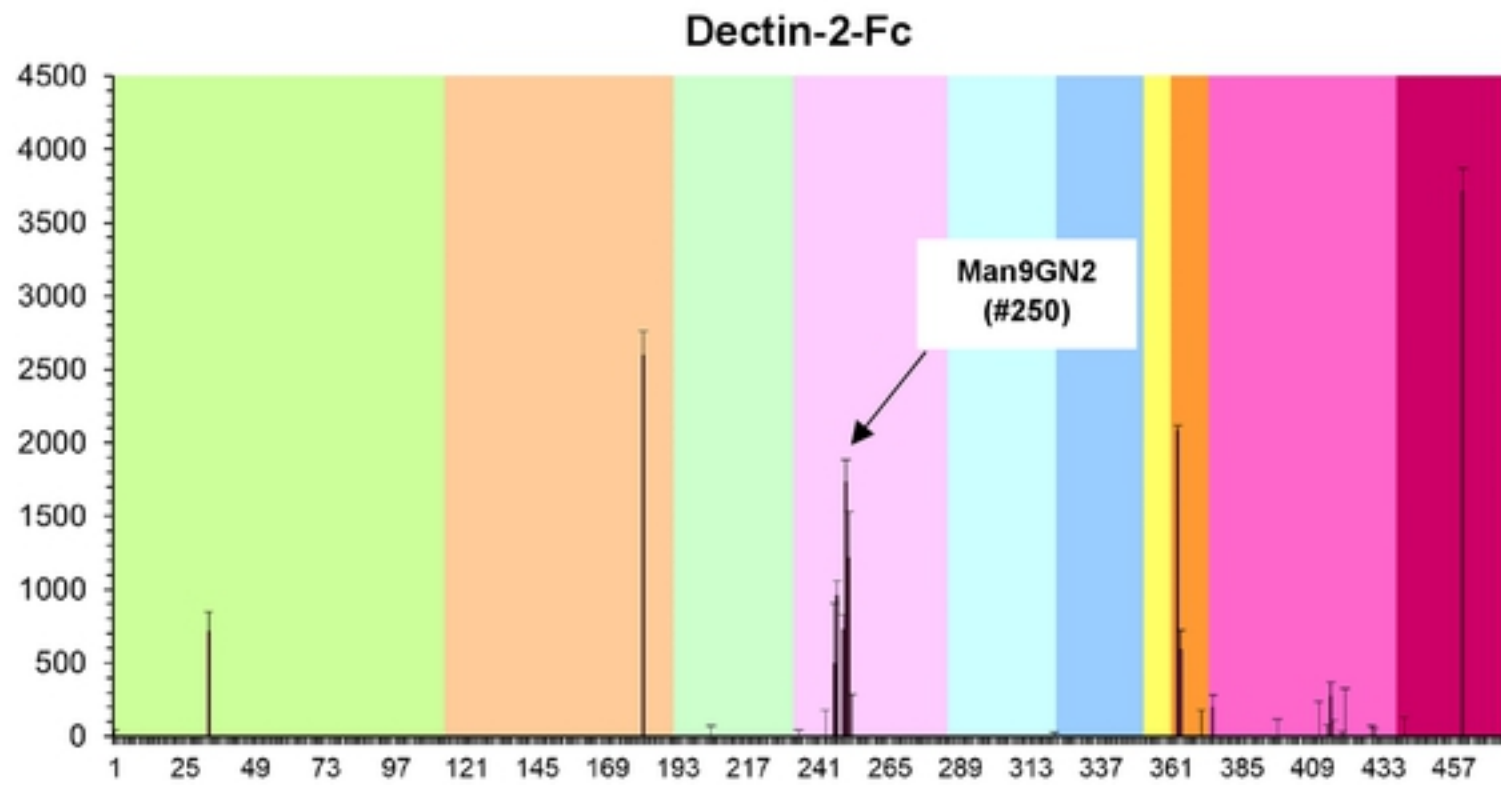
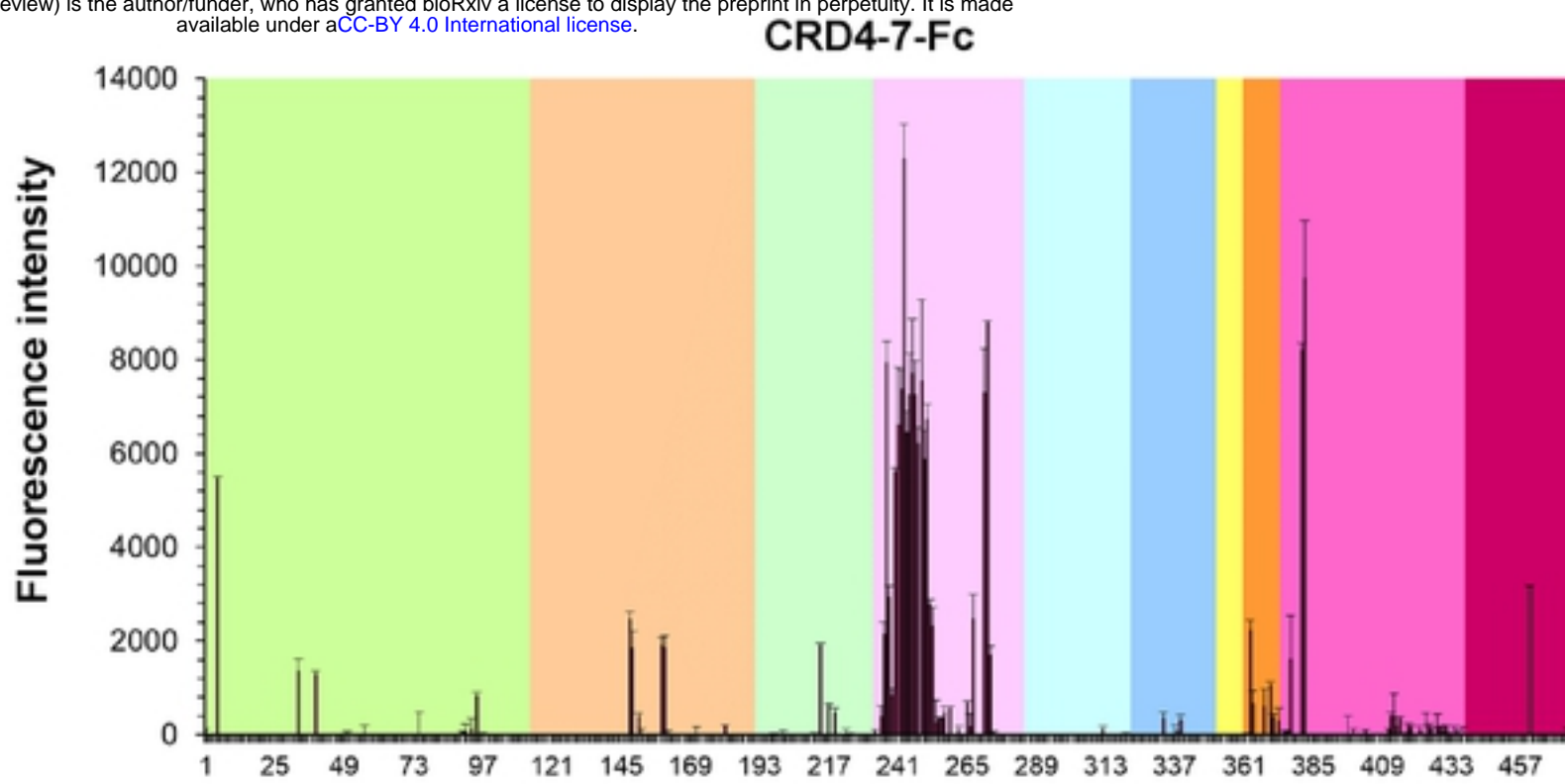
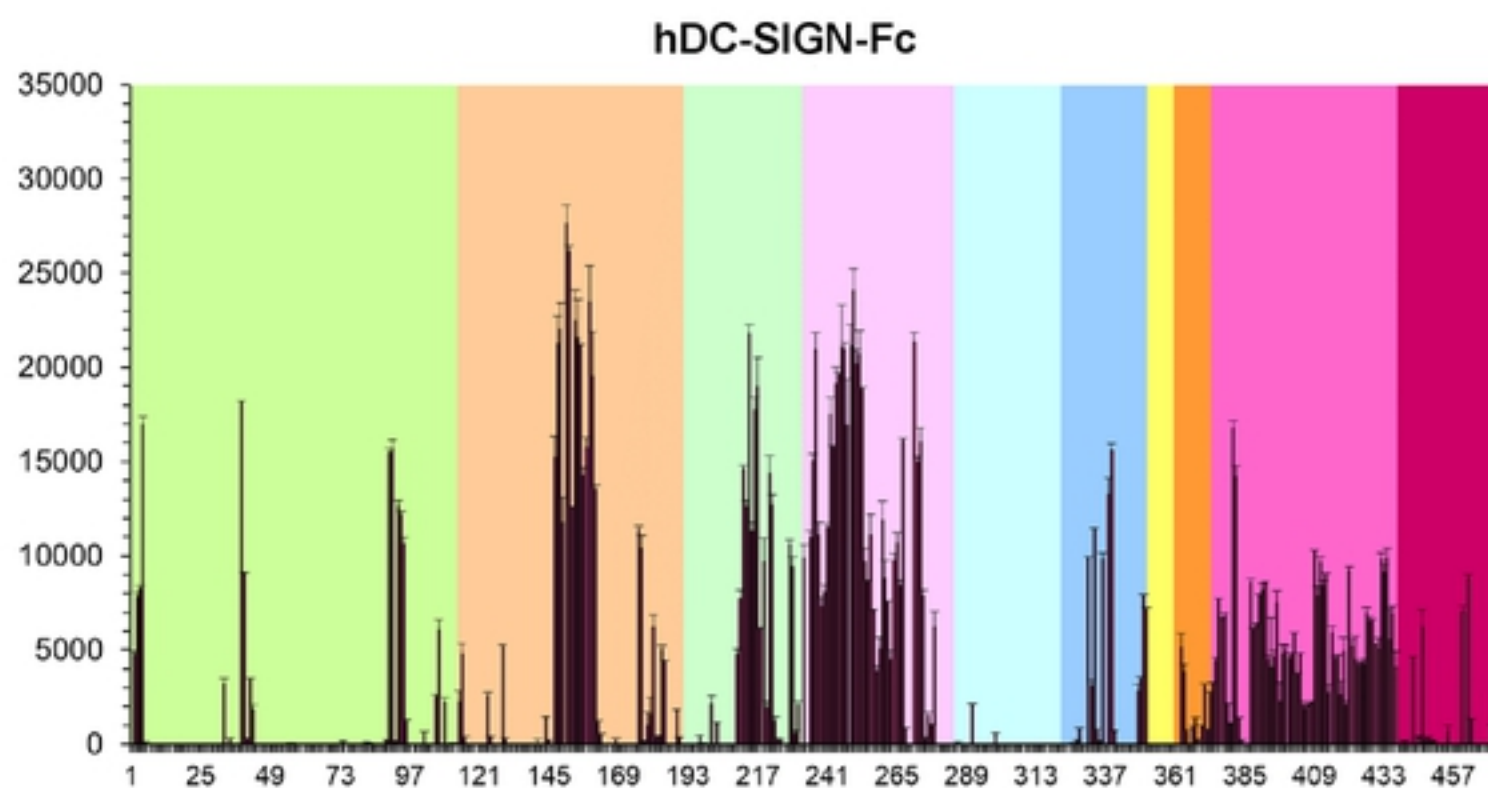


Fig. 10

A

bioRxiv preprint doi: <https://doi.org/10.1101/677104>; this version posted June 19, 2019. The copyright holder for this preprint (which was not certified by peer review) is the author/funder, who has granted bioRxiv a license to display the preprint in perpetuity. It is made available under aCC-BY 4.0 International license.

B**C**

Oligosaccharide probes

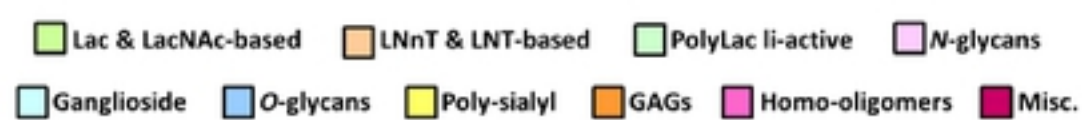
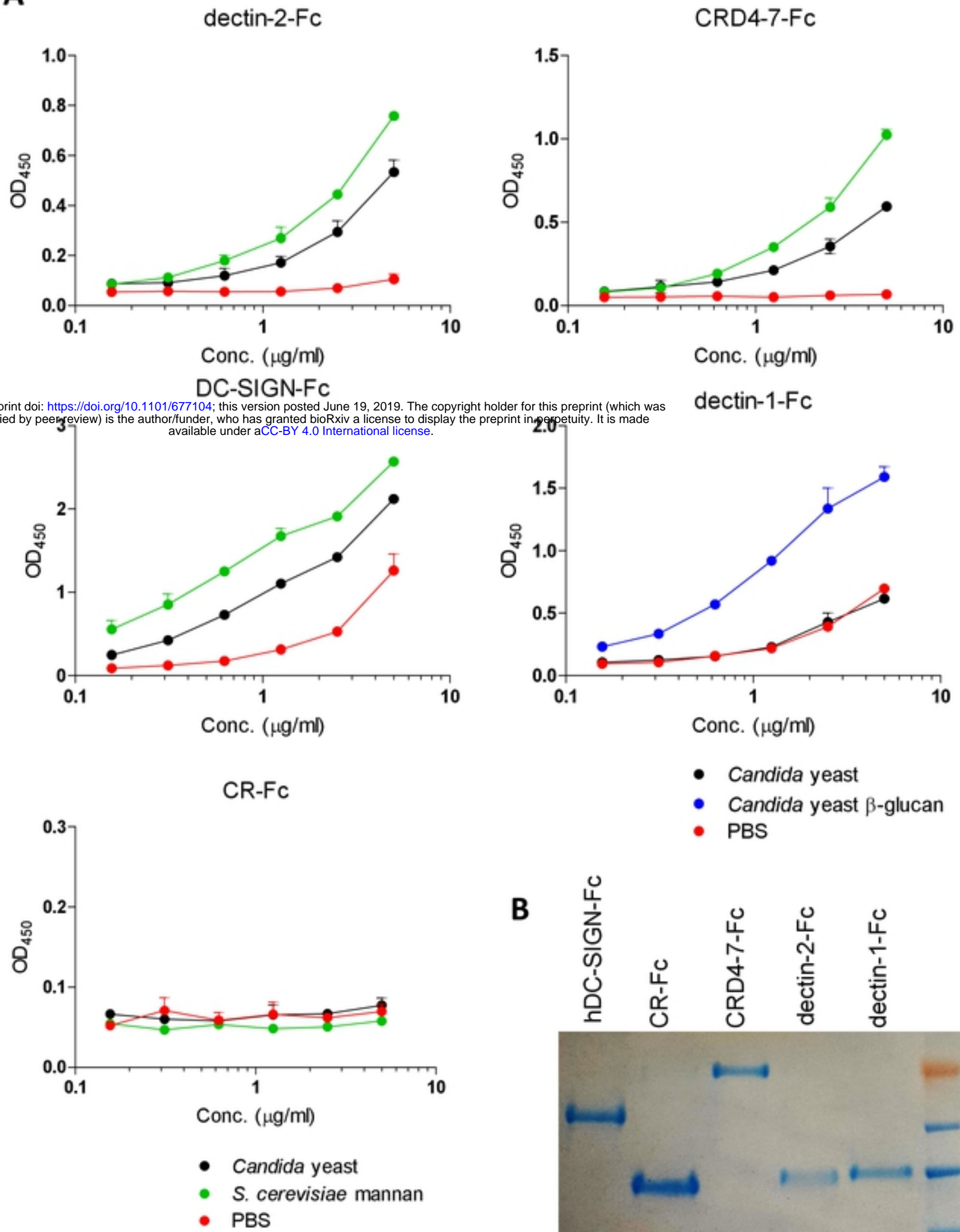
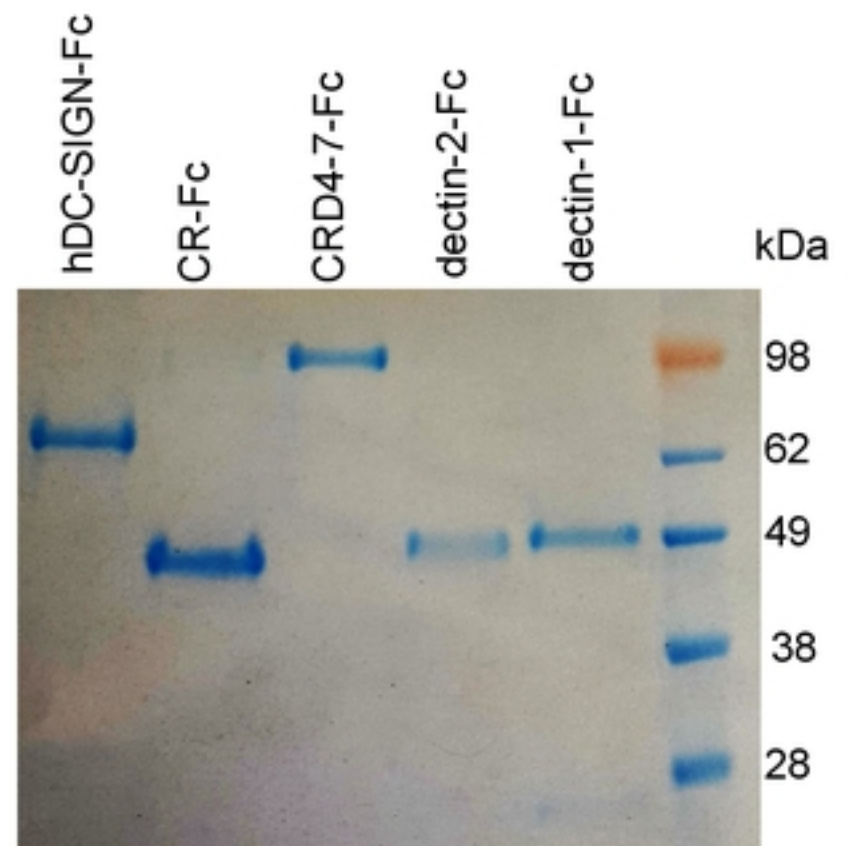


Fig. 11

A**B****S Fig. 1**